

Aus dem Institut für Medizinische Psychologie der
Ludwig-Maximilians-Universität München

Vorstand: Prof. Dr. E. Pöppel

**The circadian surface of *Neurospora crassa* -
From physiology to molecular mechanisms**

Dissertation

zum Erwerb des Doktorgrads der Medizin

an der Medizinischen Fakultät

der Ludwig-Maximilians-Universität

Vorgelegt von Jan Rémi

Geboren in Krefeld

2007

Mit Genehmigung der medizinischen Fakultät
der Universität München

1. Berichterstatter:	Prof. Dr. T. Roenneberg
2. Berichterstatter:	Prof. Dr. B. Grothe
Mitberichterstatter:	Prof. Dr. M. Meyer
Mitberichterstatter:	Prof. Dr. Chr. Lauer
Mitbetreuung durch den	
promovierten Mitarbeiter:	PD Dr. rer. nat. M. Merrow
Dekan:	Prof. Dr. med. D. Reinhardt
Tag der mündlichen Prüfung:	26.07.2007

Inhaltsangabe – Table of contents

1. Introduction:	4
1.1 Characteristics of circadian clocks	4
1.2. General properties of circadian clocks	7
1.3. <i>Neurospora crassa</i> – a molecular genetic model organism	11
1.4. <i>Neurospora crassa</i> 's clock	12
1.5. Aim of this study	17
2. Methods	19
2.1. Strains	19
2.2. Physiological methods	19
2.2.1. Strain maintenance	19
2.2.2. Race tubes	20
2.2.3. Light cycles:	24
2.3. Molecular Methods:	27
2.3.1. RNA analysis	27
2.3.2. Protein analysis	32
3. Results	38
3.1. Physiological results	38
3.1.1. Skeleton photoperiods (SPP)	38
3.1.2. The circadian surface	41
3.2. Molecular results	49
3.2.1. Choosing cycles for molecular analysis	49
3.2.2. RT-PCR results	50
3.2.3. Western blot results	54
4. Discussion	57
4.1. <i>Neurospora crassa</i> 's behavior in light-dark cycles	57
4.1.1. Entrainment to skeleton photo periods	59
4.1.2. Entrainment on a circadian surface	62
4.2. Entrainment on the molecular level	66
4.3. Does <i>Neurospora crassa</i> have an M&E oscillator?	68
5. Summary	71
6. Zusammenfassung	73
7. References	75
8. Appendix:	80
8.1. Abbreviations	80
8.2. Recipes	82
8.3. List of Instruments	84
8.4. List of chemicals	85
8.5. List of Biochemicals	87
9. Acknowledgements – Danksagung	88
10. Lebenslauf – curriculum vitae	89

1. Introduction:

1.1 Characteristics of circadian clocks

A dominant factor in the life of all organisms on earth is the alternation of day and night. With the rotation of the earth, light, temperature, food and energy supply change as well. These changes present a challenge to living systems, who could adapt to this environment by responding randomly (chaos) or by allowing simple, driven responses to occur. Rather, circadian clocks structure the biological temporal organization in response to the daily changes in the physical world. Circadian clocks confer an adaptive advantage (Johnson and Golden 1999; DeCoursey, Walker et al. 2000) and are found in all phyla, even unicellular organisms.

The alga *Gonyaulax polyedra*, as an example for single celled organisms, travels each day from the ocean's surface, where it gathers photosynthetic energy during the day, to greater depths during the night for harvesting nutrients. This migration is controlled by a circadian clock (Roenneberg and Morse 1993). Plant behavior and physiology is coordinated in circadian cycles as seen in leaf movement (Darwin 1880), cell metabolism (Lüttge 2000) and gene regulation (Bognar, Adam et al. 1999).

In mammals, rest and activity (Pittendrigh and Daan 1976a), and its extensive underlying physiological network, even circadian photoreception itself (Freedman, Lucas et al. 1999) oscillate over 24 hours. This rhythm is conducted by the supra chiasmatic nucleus (SCN), the central circadian pacemaker. Since the discovery of the SCN's function (Schwartz and Gainer 1977), the mammalian circadian system has

been explored to great depths. Mutagenesis experiments yielded animals with altered circadian properties. By now, the discovered clock genes have been put into an intricate network, revealing the complexity of the mammalian system in particular (Schwartz, Iglesia et al. 2001; Reppert and Weaver 2002) and circadian systems in general.

In humans, the specific molecular mechanisms of our circadian rhythmicity are just beginning to be explored (Hankins and Lucas 2002; Carpen, Archer et al. 2005), but the effects of the circadian clock on human physiology have been extensively described. Jürgen Aschoff, a pioneer of circadian biology in general and human circadian behavior in particular, had his subjects go through several weeks of bunker experiments in Andechs, just outside of Munich, Germany, to explore behavior without the “interference” of environmental cues (*zeitgebers*, German for “time giver”) that reset the circadian clock (Aschoff 1985). Properties of the human clock have been discovered and classified: a strictly consolidated sleep pattern (Aschoff 1965), physiological oscillation of blood pressure levels (Covic and Goldsmith 1999) and even gene expression (Ebisawa, Uchiyama et al. 2001), among others, are under control of the circadian system.

The effects of the circadian clock for humans are exemplified in jet lag (Moore-Ede 1986). Here, a desynchrony of external time cues and the timing of the body’s physiology results in the known effects: disrupted sleep patterns, gastro-intestinal afflictions, impairment of mental alertness. Now imagine being jet-lagged for most of your life, as are shift workers (Roden, Koller et al. 1993). This part of the working

population (about 20% in Germany) is challenged by the misalignment of external and internal time, as the shifts rotate on a weekly or even daily basis. The possible consequences are peptic ulcer (Reinberg, Andlauer et al. 1984), heart disease (Kawachi, Colditz et al. 1995) and even an increased risk for cancer (Schernhammer, Laden et al. 2001; Schernhammer, Laden et al. 2003). And not only workers with a classic shift work schedule, but also the daytime work force can be stressed by the misalignment of biological and social time. This effect was recently coined as “social jet-lag” (Wittmann, Dinich et al. 2005). Here the time demands of modern work and social life collide with the hard-wired biological timing of the human population.

Research incorporating circadian aspects is wide spread. But medical treatment incorporating circadian knowledge is, so far, limited to few fields: Light therapy is being applied to diseases such as seasonal affective disorders (Eastman, Young et al. 1998), antepartum depressions (Oren, Wisner et al. 2002) and sleep disorders (Terman, Lewy et al. 1995). Blind patients from certain subgroups receive melatonin treatment to entrain them to a 24 hour day, otherwise they would be freerunning (Sack, Lewy et al. 1991). Circadian timing in chemotherapy seems to be a great opportunity for improving cancer therapy (Mormont and Levi 2003), although it is yet rarely applied. Devising personalized solutions in chrono-pharmacology (for example timing of medication) and chronoecology (for example tailoring shift schedules to individual chronotypes) requires more knowledge of how to determine a person’s chronotype and what its implications are (Roenneberg, Wirz-Justice et al. 2003).

As there are many aspects of the circadian system discovered and several applications of the knowledge at hand, there are still many open questions in circadian research: the genes, proteins and interactions found so far are surely important to the clock, but there remain more to be discovered. For those identified already, their role within broad clock functions, from daily entrainment to seasonality, remains to be described.

1.2. General properties of circadian clocks

Circadian systems have been described in many model organisms. By analyzing their behavior, one can deduce properties of their clocks. Consolidating these observations allows the definition of features that are shared and which can be seen as descriptions and requirements of circadian clocks in general (Pittendrigh 1960; Roenneberg and Merrow 1998):

- Rhythmicity: An endogenous, self-sustained oscillation is observed. Examples include: gene-protein feedback loops, nervous circuits, hormone feedback mechanisms.
- Circadian range: The oscillation has a period in the circadian range. That means that one full cycle should last around 24 hours (Latin: *circa* = *about*, *diem* = *day*). Clock mutants though may have a shorter or longer period.
- Amplitude: The amplitude of the oscillation has to be large enough for experimental manipulation; it must be robust.

- Sustainability: In constant conditions (i.e. without zeitgebers) the rhythm is self sustained. It has been shown that the circadian rhythmicity is self-sustained even over years in some organisms. (Richter 1978; Gwinner 1986)
- Entrainability: Circadian systems must be synchronized to zeitgeber cycles. This process is called *entrainment* (Roenneberg, Daan et al. 2003). The organism entrains with a specific relation to the zeitgeber, called the *phase angle*. The cycles do not have to be 24 hour cycles; in fact, it is a property of the circadian organism to be able to entrain to cycles in a certain range, called the *range of entrainment*, defined by the minimum and the maximum cycle length to which the system still entrains. As an answer to very short or very long cycles, the organism can also show a *frequency demultiplication* (for example in *Neurospora*: only one 'event' every two full 12 h cycles; (Morrow, Brunner et al. 1999) or a *frequency multiplication* (two conidial bands in every full cycle; Pittendrigh and Daan 1976). Another possibility of a biological reaction to zeitgeber stimuli is drivenness. It is a reaction to a zeitgeber stimulus that is uniform in different zeitgeber conditions, and does not necessarily require a circadian clock. Entrainment differs from drivenness in being an active process where the influence of timing information on the circadian clock depends on the state of the circadian clock at the time of exposure.
- Temperature Compensation: Circadian Rhythms are highly temperature compensated, i.e. the rhythm is unchanged when different (constant) temperatures in a certain range are applied (Pittendrigh 1954). This extends to other parameters like

nutrition, social interaction or cell pH. In general it could be considered as *noise compensation*.

A conceptual approach to understanding the circadian clock is a dissection into discrete domains as shown in figure 1.1. All circadian systems consist of at least (1) a central oscillator or rhythm generator, (2) an input pathway to that oscillator and (3) an output pathway to transduce the oscillatory signal to downstream targets.

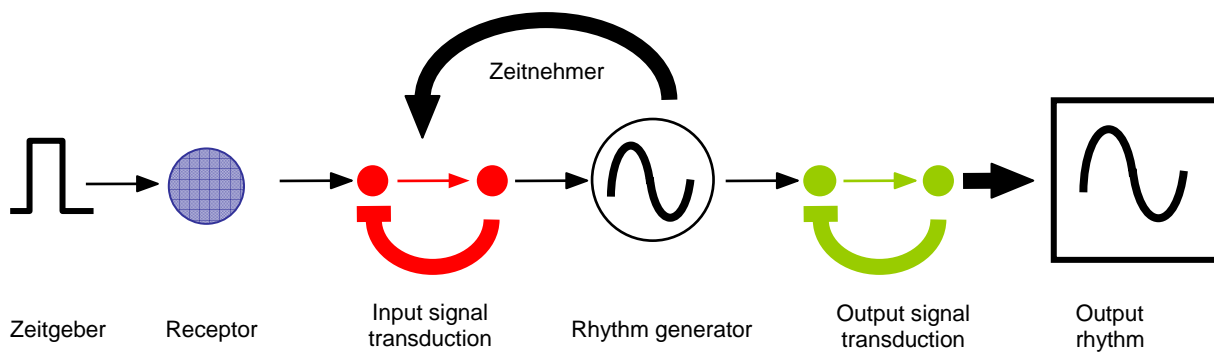


Figure 1.1.: A basic flow-chart model of a circadian pathway, already incorporating the ideas of feedback within the input and output pathways as well as feedback from the central oscillator to the input pathway (*zeitnehmer*).

To further illustrate the basic three components of the circadian clock, an example of each will be described shortly with an emphasis on the oscillator:

(1) Input pathway: The most important input to the circadian clock in most organisms is light. Its receptor has requirements that make it special and different from visual photoreception. Where photoreception for vision must be fast (high time resolution) and accurate (high spatial resolution), circadian photoreception should

only integrate amounts of light over the course of the day, just like a scintillation counter (Roenneberg and Foster 1997; Roenneberg and Merrow 2000; Hattar, Liao et al. 2002). After the receptor has been activated by the zeitgeber signal, the information is then passed to the oscillator, for example by axonal conduction in mammals from the retina to the supra chiasmatic nucleus - the central oscillator (Berson, Dunn et al. 2002; Menaker 2003).

(2) Central oscillator: The SCN as the most prominent example for a circadian oscillator, is made up of neurons that, when dissociated, display a circadian rhythm in multi unit activity (Welsh, Logothetis et al. 1995). Thus, each of these cells, receiving information about the state of the light environment, is a unit of the circadian oscillator. One of the existing theories about the molecular mechanism of circadian rhythm is that it consists of a single Transcriptional-Translational-feedback-Loop (TTL). In *Neurospora crassa* for example, the negative element FREQUENCY feeds back via the WHITE-COLLAR-COMPLEX (WCC) to an element in the promoter region of the *frequency* gene itself (Denault, Loros et al. 2001). But there are open questions: How does a single TTL slow down to a circa 24 hour period? A gene-protein feedback loop can take less than 4 hours (Allada 2003). Recent modeling shows that the circadian clock could consist of several short period TTLs that, when forming a network, result in a freerunning period (FRP) of around 24 hours. That model has all the necessary properties mentioned above. It is also conceptually attractive to model the evolution of circadian clocks as a connection of already existing TTLs and not a newly evolved one (Roenneberg and Merrow 2002).

(3) Output pathway: An example for the output pathway in mammals is the induction of the VIP-gene (Silver, Sookhoo et al. 1999; Hurst, Mitchell et al. 2002). VIP, as well as other neuropeptides (vasopressin, cholecystokinin and substance P), has a regulating E-Box element in its promoter. These genes are used as readouts for circadian activity and are represent an example of direct clock control. Next to VIP and other neuropeptides, direct genetic clock control over more than a hundred genes has already been shown (Oishi, Miyazaki et al. 2003), and the control of many more is suspected.

1.3. *Neurospora crassa* – a molecular genetic model organism

When trying to understand different aspects of a system, the use of different model organisms has proved to be a valuable tool. In this thesis, the pink bread mould *Neurospora crassa* (see fig 1.2. for electron microscopy pictures) has been used to investigate entrainment properties of the circadian system. *Neurospora*, which was the tool to discover the “one gene - one enzyme” hypothesis, is an excellent research tool for several reasons: tissue can be grown in a few days, sometimes even hours; it has a haploid genome, making reverse and forward genetics easier than in diploid organisms; it offers a wealth of well developed genetic and biochemical tools, enabling widespread research.

Its genome is fully sequenced (Galagan, Calvo et al. 2003), making molecular research even more systematic and mutagenesis experiments easily referenced.

Neurospora is also very well suited for observing circadian physiology. For its circadian output behavior, there is an obvious and convenient marker: conidial banding. As part of its life cycle it produces asexual spores, called conidia, and it does so with a distinct phase relationship to external time (Roenneberg and Merrow 2001).

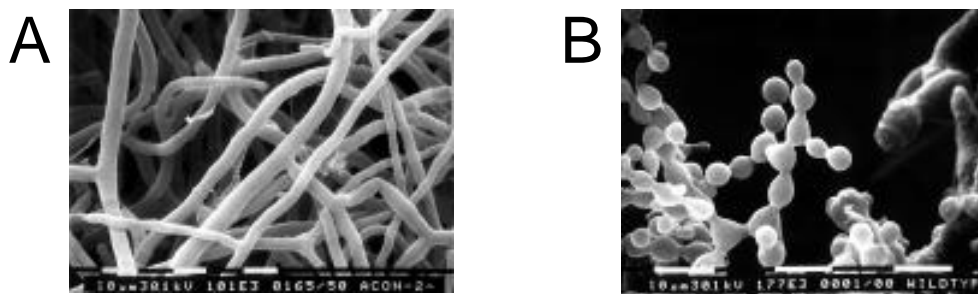


Figure 1.2.: Electron microscopy showing developmental forms of *Neurospora crassa*. (A) vegetative form with aerial hyphae. (The actual picture shows *aconidiate-2*, a mutant that doesn't produce conidia.) (B) macroconidiophores or conidia after septation and some separation. Some regions of aerial hyphae are also visible. (pictures from Dr. Matt Springer, Fungal Genetic Stocks Center, www.fgsc.net)

1.4. *Neurospora crassa*'s clock

Neurospora crassa shows robust, self-sustained rhythmicity in constant darkness (DD), but not in constant light (LL). Under that condition, the free-running period (FRP) of the wild type is approximately 22 hours. The FRP can be altered by mutations of the clock gene *frequency* (*frq*), which was discovered itself in a mutant screen (Feldman and Hoyle 1973). Null mutants of the frequency gene are arrhythmic, except when exposed to very special conditions (Loros and Feldman

1986; Aronson, Johnson et al. 1994; Roenneberg, Dragovic et al. 2005). The expression levels and ratios of the long (l) and short (s) isoforms of the protein FREQUENCY (FRQ) are, furthermore, crucial for the good temperature compensation of *Neurospora crassa*. The ratio of l-FRQ versus s-FRQ is regulated by thermo-sensitive splicing of intron 6 of *frq*, allowing adjustment of FRQ levels according to ambient temperature (Liu, Garceau et al. 1997; Diernfellner, Schafmeier et al. 2005). The FRQ protein is the central element of a negative feedback loop, with a negative feedback on its own transcription, and furthermore inhibiting the promoting effect of the WHITE COLLAR Complex (WCC) on *frq* transcription (Lee, Loros et al. 2000). On the other hand, FRQ promotes the transcription of *wc-1*, thus enhancing the amount of WCC (Schafmeier, Haase et al. 2005). The FRQ-WCC feedback loop is so far the only oscillator with known components.

Next to the FRQ-WCC feedback loop, a multi-oscillator circadian system is revealed by rhythmicity in *frq* knockout strains and the required components are termed the "FRQ-Less-Oscillator" (FLO). It seems to be coupled to the FRQ/WCC feedback loop. Its existence has been shown, yet specific components have not been described so far (Loros and Feldman 1986; Merrow, Brunner et al. 1999).

As a circadian clock gene, *frq* is regulated under the influence of zeitgebers, the most important being temperature and light, with the light input requiring photoreceptive structures. In *Neurospora crassa*, WC-1 is a blue-light receptor that mediates the induction of many light inducible genes (Lee, Dunlap et al. 2003). Along with its partner WC-2, WC-1 is required for self-sustained rhythmicity in constant

conditions (Crosthwaite, Dunlap et al. 1997). As mentioned above, the WCC binds to the *frq*-promoter at two sites, enhancing transcription (Froehlich, Liu et al. 2002). Whereas WC-1 is a photoreceptor, WC-2 is an important mediator for protein interaction (Loros and Dunlap 2001). Although WC-1 is so far thought to be the only photoreceptor, it has been shown functionally that light responses involve other light receptors (Dragovic, Tan et al. 2002), as also suggested by the genome sequence (Galagan, Calvo et al. 2003).

Adding more complexity, Schwerdtfeger and Linden showed that the VIVID-protein (VVD) is also a blue light photoreceptor, which gates light input to the system, by interacting with other proteins via its PAS domain (Schwerdtfeger and Linden 2003). *vvd*-null strains show robust rhythmicity (Heintzen, Loros et al. 2001). Finally, a *Neurospora* opsin-like protein (NOP-1) was shown to have green light photoreception by expressing it in the yeast *Pichia pastoris* (Bieszke, Spudich et al. 1999). This protein has no demonstrable function in *Neurospora* as yet.

Our group was able to show entrainment of *Neurospora* in temperature cycles (22°C – 27°C T-cycles, where cycle length is varied to explore entrained phase relationships). When light was used as a zeitgeber in symmetrical cycles of varying lengths, *Neurospora crassa* seemed to be driven by full photoperiods, rather than being entrained by them (Merrow, Brunner et al. 1999; see section 1.2 for further explanation of entrainment and drivenness). Subsequent entrainment experiments with various photoperiods in the context of T = 24 h showed non-driven responses

(Tan, Dragovic et al. 2004) leaving room for the experimental setup of this thesis (see section 1.5).

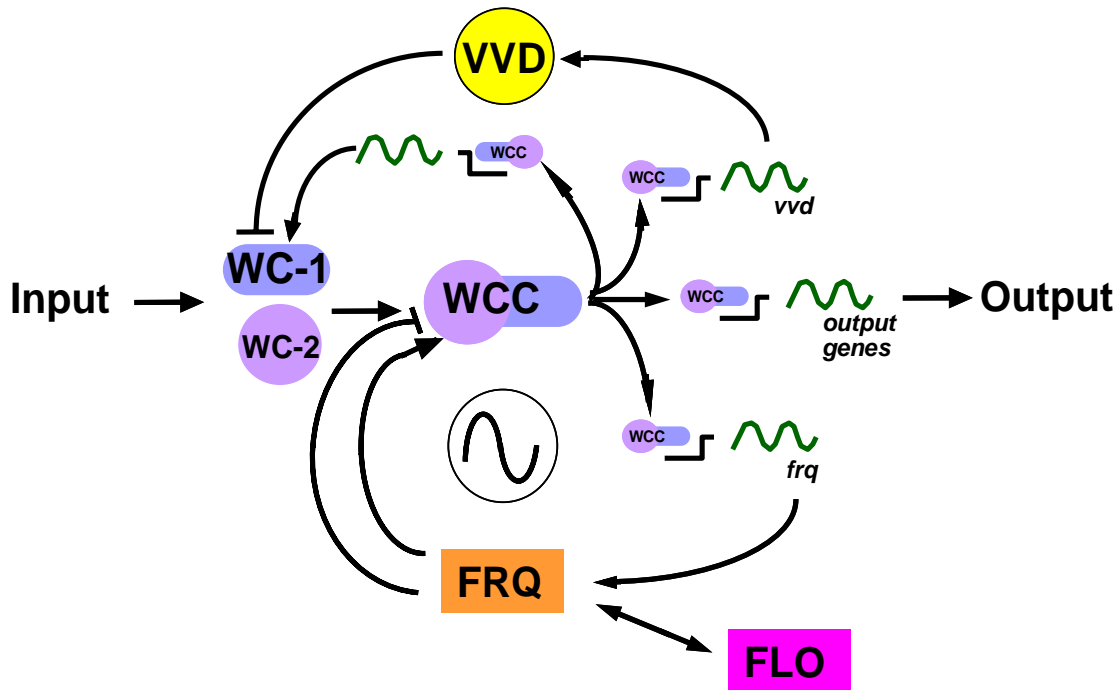


Figure 1.2.: The levels of *frequency* (*frq*) RNA and FRQ protein depend on WHITE-COLLAR-1 (WC-1) and WC-2, which heterodimerize to form the White Collar Complex (WCC). WC-1 levels depend on FRQ. In constant darkness, expression of FRQ protein results in reduced *frq* RNA accumulation. The net effect is two interlinked regulatory loops. Light reaches the system through the WCC, which is essential for light responses in *Neurospora*. VVD gates the light input to the system by interaction with WC-1. *ccgs* are clock-controlled-genes, some of which are light induced. The FLO (*frq*-less-oscillator) has been shown to exist, but components have not yet described (Merrow, Brunner et al. 1999), (Loros and Feldman 1986). (Redrawn from (Heintzen, Loros et al. 2001))

Earlier, the acute induction of *frq* RNA by light, referenced to changes in the phase angle in concomitant physiological experiments, led to a hypothesis for a molecular entrainment mechanism: Resetting of *frq* mRNA, and with it FRQ protein

levels, resets the circadian clock to the circadian time of day for which *frq* expression is typical (Crosthwaite, Loros et al. 1995). Our group has shown, however, that the peak in *frq*-RNA expression and the peak of FRQ-protein accumulation under different photoperiods can be independent (Tan, Dragovic et al. 2004). Thus, entrainment is obviously more complex than just a reset of the clock correlating with the peak of mRNA expression.

A model of *Neurospora crassa*'s clock, as conceived so far, is shown in figure 1.2, summing up the above mentioned information.

1.5. Aim of this study

Although circadian rhythms are extensively documented in free running conditions at all levels – from genes to behavior – relatively few experiments applied entrainment protocols, despite the fact that entraining conditions are the typical environment for a functioning circadian clock. So, research on entrainment in an excellent molecular model organism is the next step in understanding circadian behavior after the successes in research of the free-running period.

Two different fundamental protocols were used in this study: Skeleton and full photoperiods. Skeleton photoperiods are light-dark cycles, where two light pulses are used to mimic dusk and dawn, i.e. a “skeleton” day.

We coined the term “circadian surface” to describe an extensive set of experiments where three variables are changed systematically: (1) the length of zeitgeber cycles (T; for example: light-dark cycles or cold-warm cycles), (2) the proportion of the two phases (i.e. light or dark in photoperiod experiments) and (3) the free-running period (FRP) of the studied strains. The latter were not changed as part of the experiment, but rather were the strains selected for the experiments on the base of their respective FRP.

Previous experiments applying surface-like experiments were mostly aimed at revealing photoperiodic properties of the respective organisms. They showed highly systematic responses to the different zeitgeber cycles. This study is the first time that a complete circadian surface was compiled for any model organism.

The questions that are addressed with this study are:

- (1) What are the rules of entrainment by light for *Neurospora*?
- (2) When the physiological behavior reveals entrainment, how does the critical clock gene *frq* (frequency) behave in its molecular profiles?

2. Methods

2.1. Strains

For circadian research *Neurospora crassa* strains with the band (*bd*) mutation are commonly used. This mutation allows an analysis of conidial banding in race tubes, which, in the wild type strain, is weak, presumably by a suppressive effect of accumulating CO₂ in the race tube (Sargent and Kaltenborn 1972).

For this study the following strains were used:

- *bd a 30-7*, the standard lab strain with only the *bd* mutation, showing a free running period (FRP) of approximately 22h. (abbrev: *frq*⁺)
- *bd frq*¹, a short period mutant (FRP ≈ 16h). (abbrev: *frq*¹)
- *bd frq*⁷, a long period mutant (FRP ≈ 29h). (abbrev: *frq*⁷)

Both *frq*⁷ and the *frq*¹ mutations are single point mutations (transition G to A) in the *frequency* gene (Merrow and Dunlap 1994).

2.2. Physiological methods

2.2.1. Strain maintenance

The strains used for stocks were inoculated to reagent tubes with slanted Vogel's minimal agar medium (slants), then allowed to develop on the bench for 7 days, covered with parafilm and then frozen to -20°C.

The strains for working stocks were kept at 4°C in the dark in minimal medium slants, and discarded two months after inoculation.

The experimental conidia came from working cultures, about seven days old, kept at room temperature in minimal medium slants.

To produce conidial suspensions for inoculation of liquid medium, 1000ml Erlenmeyer flasks with 200ml of race tube medium were inoculated from stock and allowed to grow for 14 days at room temperature. They were then rinsed with approximately 100ml of sterile H₂O, filtered through sterile gauze, filled to sterile bottles and shaken to make a homogeneous suspension. The concentration was determined by optical density at 420nm.

2.2.2. Race tubes

2.2.2.1. Race tube setup

For monitoring physiological responses to experimental conditions so called race tubes were used. Race tubes are glass tubes about 30 cm long with a diameter of 1.3 cm, each end turned up by approximately 35° to allow filling (race tubes are produced by companies Höhn, Munich and Schmitz, Munich). The single race tubes were tied together to three-packs or six-packs to allow easier handling. The race tubes were filled with 6 ml of hot, liquid race tube medium (see appendix for all recipes). After autoclaving, the ends were sealed with sterile plugs to prevent contamination. The cooled race tubes were inoculated with a loop of conidia from working slants at one of the ends. They were allowed to germinate in constant light

at room temperature for 24h. The growth front was then marked and they were transferred into their respective experimental setup. During the experiment the growth front in each tube was marked every other day to allow referencing experimental time points to the presented phenotype. See fig 2.1. for an example of a sixpack of racetubes.

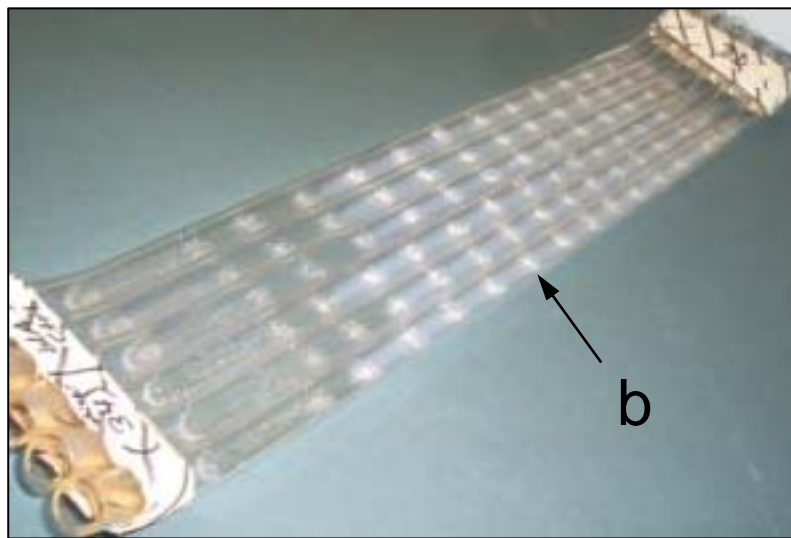


Figure 2.1: Photograph of a sixpack of racetubes with the typical conidial banding pattern across the length of the racetube (**b**: single conidial band).

2.2.2.2. Race tube analysis

To allow easy analysis, the race tubes were scanned (AGFA Snapscan 1236, settings: grayscale, 150 dpi). Then the optical density, changing with conidiation and mycelial growth, was determined at every 10 minute time point with the image analysis section of the *Chrono* program (Prof. T. Roenneberg, LMU). The resulting series of optical densities was plotted as a function of time (fig. 2.2).

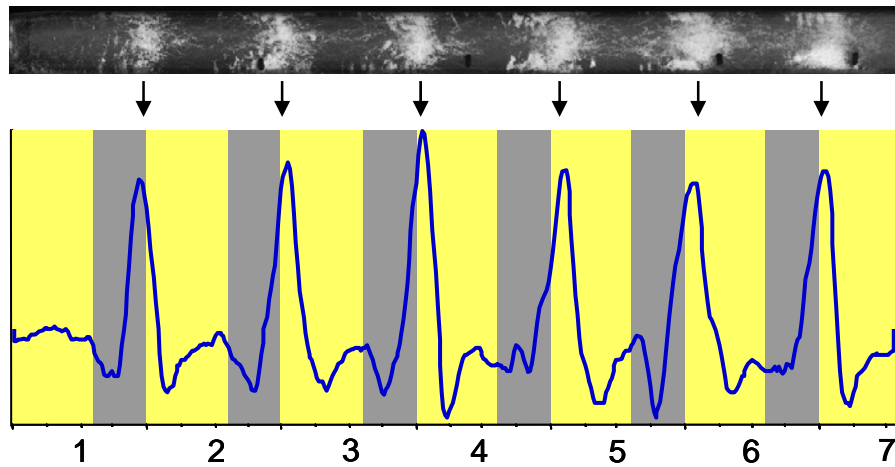


Figure 2.2: Here the conversion from the scanned picture to a line graph of optical density (y-axis) over time in days (x-axis) is shown.

To be able to see changes in the conidiation pattern over time, the experimental days were plotted in rows beneath each other. To follow conidiation more easily across the dateline, two single plots were fused to a double plot (fig 2.3).

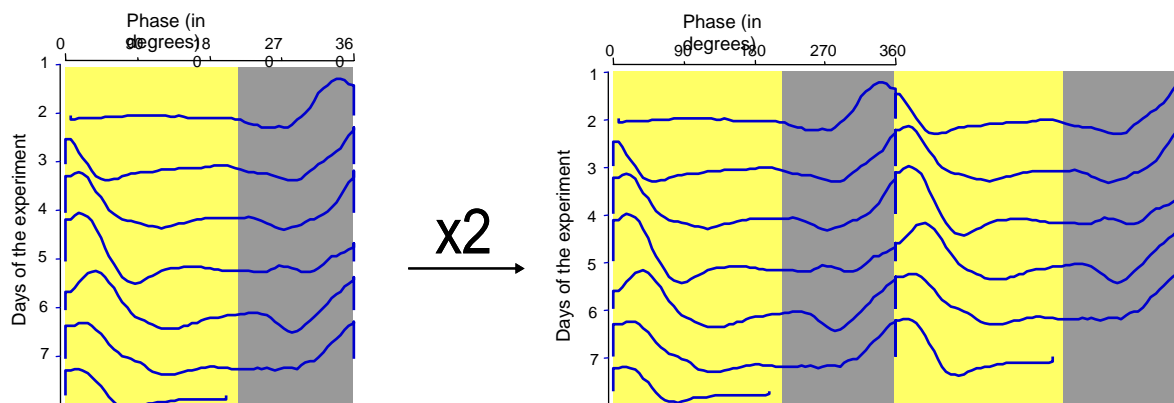


Figure 2.3: The daily pattern of conidiation is plotted day under day. For better analysis, two single plots are fused to a double plot.

To analyze the average onset, peak and offset of conidiation, a composite graph was used as shown in figure 2.4. Here, the average of the days 2 to the last but one was used to compile the Composite Curve. (Day 1 was left out, because *Neurospora* had not yet reached a stable phase angle. The last day was left out, because at the end of the racetube, the reading for optical density is often not exact.)

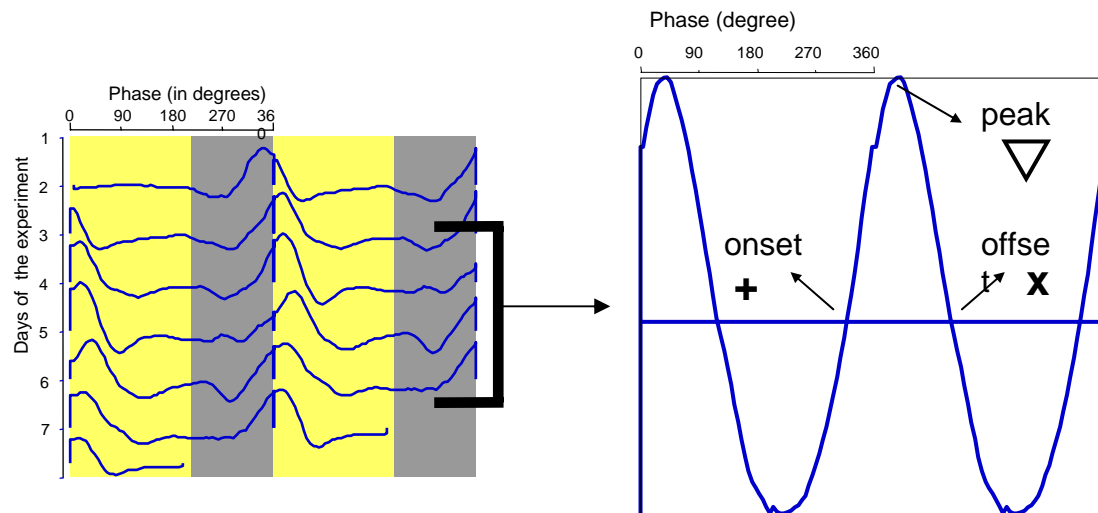


Figure 2.4: The *Chrono* program allows averaging curves over several days. By compiling the entrained days of the experiment to a Composite Curve, it is then easy to read out the peak of conidiation and the onset and offset of conidiation, both defined as the transition point through the daily average (blue horizontal line).

To analyze the average onset, peak and offset of conidiation, a composite graph was used as shown in figure 2.4. Here, the average of the days 2 to the last but one was used to compile the Composite Curve. (Day 1 was left out, because *Neurospora* had not yet reached a stable phase angle. The last day was left out, because at the end of the racetube, the reading for optical density is often not exact.)

From the composite curve, the times of onset, peak and offset - in relation to the first lights on signal - were read into a spreadsheet to plot all light conditions for one T-cycle onto one graph. The arithmetic mean for the Composite Curves of all the race tubes (numbering six to fifteen racetubes per condition) for that one condition was calculated. The data is expressed in degrees, whereby the 24 hour day is divided into 360 degrees, to enable easier comparison of cycles that differ in length. See figure 2.5 (The results from the example race tube are encircled).

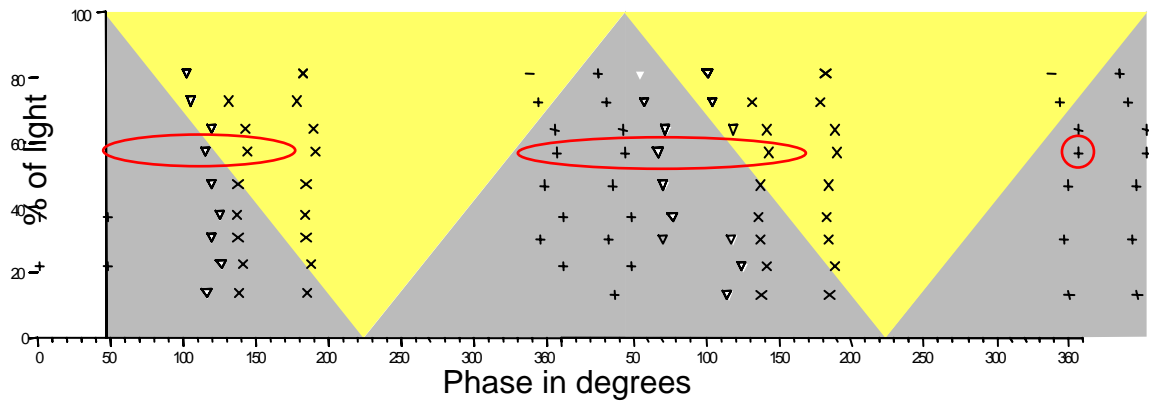


Figure 2.5: A double plotted depiction of the conidiation pattern (+ = onset, Δ = peak, x = offset of conidiation) in a given T-cycle. Here, all 9 different photoperiods are plotted together in one graph, allowing analysis of the conidiation pattern. (The condition from the example in figs. 2.1., 2.2. and 2.3. is encircled.)

As the 0 degree reference point, midnight was used. If lights on were chosen as the 0 degrees reference point, the results would remain the same, but they are easier to interpret with midnight as the reference. (See results figs. 3.4. - 3.21.) It is also easier to follow, because it corresponds more readily to clock time, where midnight is 0:00 h (Daan, Merrow et al. 2002)

2.2.3. Light cycles:

To perform the light-dark cycles experiments, light boxes had to be especially designed and produced, to enable the very high amount of experimental conditions in this thesis: 6 different cycle lengths with 9 different amounts of light-dark each for 3 different strains result 162 different conditions for the circadian surface physiology alone. For the skeleton photo periods, another total of 66 conditions were added. Considering the 3 - 4 repetitions that were done for each condition, this results in a total of 700-800 experiments done (with 6-12 racetubes in each experiment), not yet

considering the darkness-only controls - which were done in light tight aluminum boxes - and the about 50 experiments for molecular results.

The lab's facilities for light-dark racetube experiments were so far 3 separate rooms, enabling 3 different setups at one time. Considering the average experiment duration of 6-10 days, the experiments would have taken several years. Therefore, I built 15 light-tight boxes (see figs. 2.6 and 2.7). The boxes had a fluorescent light source (OSRAM Dulux L, 10W), producing $3.5 \mu\text{E}/\text{m}^2/\text{sec}$ at the box's floor level (fluency was measured with an IL1400A Photometer, International Light). The light in each box can be switched on and off with a computer interface independently from other boxes, allowing up to 15 different experimental light conditions at a time. The light within the boxes is homogenized by mirrors and a diffuser pane (Cinegel #3026, Rosco), giving an even light distribution at the box's floor. The boxes are set up in a climatized room ($25^\circ\text{C} \pm 0.5^\circ\text{C}$), with the temperature change being even less within the boxes. The minimal amount of heat produced by the fluorescent bulbs was fanned away with 10W computer fans (Philipps). The light cycles were controlled with a computer program (Roenneberg, Munich) that allows graphical control of On/Off cycles by transducing low voltage computer I/O signals via a switch box into 220V current flow to the light sources.

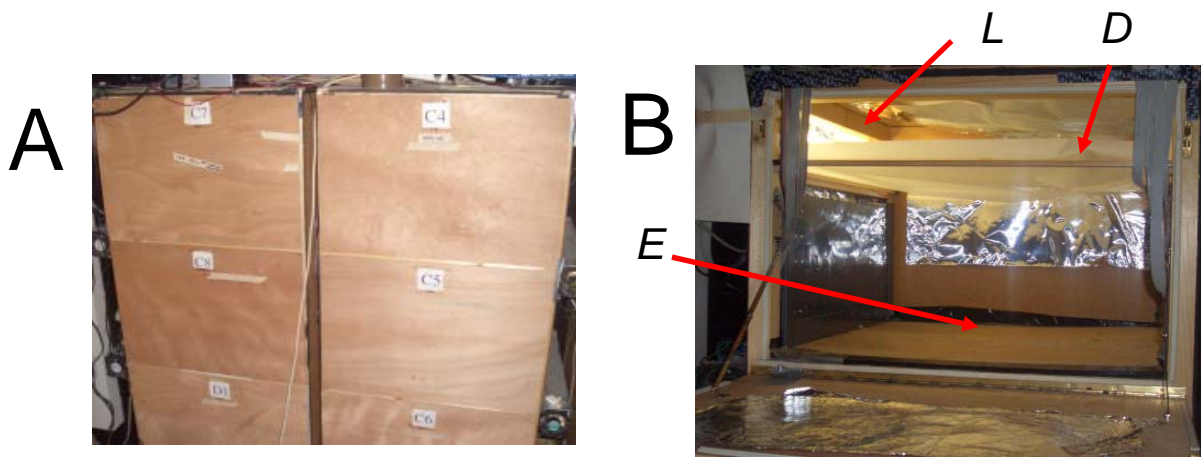


Figure 2.6: Photographs of the light boxes. **A:** Six of the 15 light boxes. Lighting was only turned on for the photograph. **B:** One of the light boxes with an open door. Italic letters denote: *L* light source, *D* diffuser pane, *E* experimental area (50x40cm) with even light distribution

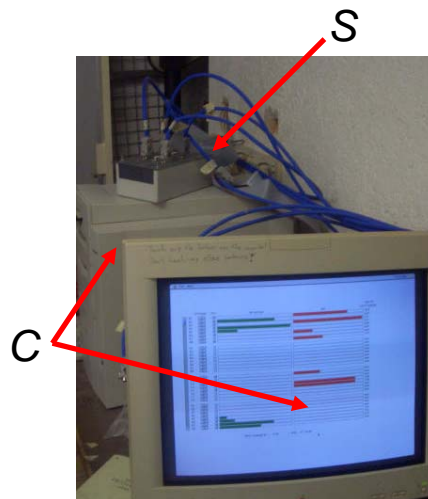


Figure 2.7: Photograph of the control room with the computer interface to control cycles within the boxes. Italic letters: *C* Computer and screen with On/Off control program, *S* switch box, changing the computer's I/O signals into electrical current I/O.

2.3. Molecular Methods:

To produce tissue for molecular analysis, mycelial mats were grown in liquid culture. For that purpose, sterile Petri dishes (60 mm diameter) containing 10 ml of liquid Vogel's medium were inoculated with approximately 10^6 conidia and immediately transferred into their experimental condition. The mats were quickly harvested by press-drying with paper towels, stored in 1.5 ml Eppendorf tubes and deep frozen in liquid nitrogen. Samples were stored at -75°C for subsequent processing.

2.3.1. RNA analysis

2.3.1.1. RNA extraction

1. Extraction

The frozen tissue was ground in a nitrogen cooled mortar with a pestle and approximately 100 μl of sand, then immediately filled into a 1.5 ml Eppendorf tube, containing 500 μl of Phenol and 600 μl of RNA extraction buffer. The tube was vortexed and then shaken vigorously at room temperature for up to 30 minutes and during that period vortexed three additional times. Centrifuging for 20 min at 14,000g, 4°C followed.

2. Cleaning

The clear supernatant was pipetted into a tube containing 500 μl Chloroform: Isoamyl alcohol (24:1), being careful that none of the dividing layer was sucked into

the pipette. The tube was vortexed 3 times, every 5 minutes, and then centrifuged briefly.

3. Precipitation

The supernatant after centrifuging in step 2 was pipetted into a tube containing 1/10 Vol (of step 2 supernatant) of 3M Na-Acetate and 2 Vol (of step 2 supernatant) of ice cold Ethanol (100%). The tube was shaken gently, put on ice for 10 minutes and centrifuged for 10 minutes at 14 000 g, 4°C. The supernatant was poured off, the remaining supernatant pipetted off and the cup left open to dry if necessary, to result in a dry RNA pellet.

4. Resuspension

The precipitated RNA/DNA pellet was resuspended in 100 µl of RNA-Secure 1X and shaken at 4°C for 10 minutes. When the RNA/DNA was fully resuspended, step 5 was carried out.

5. Aliquoting

The tube was centrifuged shortly, and divided into three: 55 µl in a stock tube, 20 µl in an aliquot tube for measuring RNA concentration and 15 µl in a RT-tube for eventual reverse transcription.

2.3.1.2. Quantification

The aliquots of the samples (see step 5 in “RNA extraction”) were diluted to 1:250. The RNA concentration was then determined by optical density (Ultrospec™ 3100 pro, Biochrom) at a wave length of 260 nm. A solution containing 40 µg/ml

RNA has an absorption of $A = 1.0$ at 260nm, when measured in a cuvette with a path thickness of 10 mm. In addition to the measurement of the concentration with 260 nm UV-light, the quality of the RNA extraction was checked with a measurement at 280 nm. The ratio of $\text{Absorption}_{260\text{nm}}/\text{Absorption}_{280\text{nm}}$ is 2.0 for pure RNA. Another measurement at 320 nm checked for protein contamination. If the OD_{320} was below 0.01, the sample was virtually protein free.

2.3.1.3. Reverse Transcription

For Real Time PCR, the RNA has to be reverse transcribed to cDNA. To prevent false results from genomic DNA, the first step is to digest the contaminant DNA. 10 μl of the RNA sample (0.2 $\mu\text{g}/\mu\text{l}$) were mixed with 10 μl of the DNase premix. The Premix contained 1X DNase I buffer, 10 U/ μl DNase I enzyme (amplification grade) and ddH₂O for a total volume of 20 μl . The mixture was incubated at 25°C for 10 minutes, followed by 10 minutes at 65°C. For reverse transcription the resulting DNA-free sample was then mixed with the Reverse Transcription (all reagents for reverse transcription from “TaqMan® RT Reagents” and “AmpliTaq Gold® PCR Master Mix” kits, Applied Biosystems) premix. The premix contained:

- 1X TaqMan® RT buffer
- 500 μM of each dNTP
- 5.5mM MgCl
- 40 U RNase inhibitor
- 125 U Reverse Transcription enzyme
- 2.5 μM oligonucleotides (rN6/d(T)16/Spec.

The reverse transcription then went through a three step incubation: 10 minutes at 25°C, 30 minutes at 42°C and 5 minutes at 95°C. After reverse transcription, the samples were diluted 1:2 with RNase free water.

2.3.1.4. Real Time PCR

Determining amounts of mRNA at distinct points of the circadian cycle is a crucial tool to approach the kinetics of the molecular components of a circadian clock. An excellent tool, allowing analysis in short time, is Real Time PCR. For analysis in this study, the Applied Biosystems ABIPrism 7000 Sequence Detection System was used.

As the reporter, SYBR Green PCR Master Mix (Applied Biosystems®) was used as the fluorescent dye. The primers (from Metabion, Germany or from SigmaArk, Germany®) and their sequences are listed in table 2.1. The final volume in each well was 25 µl. The thermocycler was set to run a three stage program:

- Stage 1: 50°C for 2 minutes
- Stage 2: 95°C for 10 minutes
- Stage 3: 40 cycles of: 95°C for 15 seconds, followed by 60°C for 1 minute.

When the program was finished, the results section of the ABIPrism program was checked to verify that the experiment was of high quality (smooth dissociation

curves, clear sigmoid shape of the dissociation curve and comparison of the triple repeats), and then saved to an export file to allow further analysis in Microsoft Excel.

Table 2.1: Sequences of the primers used in the RT-PCR

Product:	Sequence of the primer:
Ribosomal 26s FO	AGC GGA GGA AAA GAA ACC AAC
Ribosomal 26s RE	CGC TTC ACT CGC CGT TAC TAG
frq-FO sy1	CGC CTT GCG CGA GAT ACT AG
frq-RE sy1	TCC CAG TGC GGA AGA TGA AG
wc-1 sy2 FO	CCG ACT GGC ACA AAC AAT CC
wc-1 sy2 RE	CGT CTG CGT TCT CAA AAA GC
vvd FO;sy1	GAC ACG TCA TGC GCT CTG AT
vvd RE;sy1	TGG CGT GTC TTT TTG CTT CA

2.3.2. Protein analysis

2.3.2.1. Protein extraction

The frozen tissue was ground in a nitrogen cooled mortar with a pestle and approximately 100 μl of sand, then immediately filled into a 1.5 ml Eppendorf tube, containing 50 μl of Protein extraction buffer (PEB). The amount of the sample added was about equal in volume to the buffer. To prevent proteolysis 10 $\mu\text{g/ml}$ leupeptin, 10 $\mu\text{g/ml}$ pepstatin and 1mM PMSF was added to the PEB just before the extraction. The samples were kept on ice for 20 minutes and were vortexed 3 times during that period to ensure a high yield. They were then centrifuged at 14,000 rpm, 4°C for 25 minutes. The clear supernatant was then carefully pipetted into another tube, making sure that neither the solid layer underneath it, nor the thin lipid layer on top of it were taken. The extract was then stored at -75°C until further analysis.

2.3.2.2. Quantification

For quantification 10 μl of a 1:10 dilution of the samples was mixed with 1ml of the Bradford Assay Premix (Biorad) and referenced to a standard curve by optical densimetry at 595nm (Ultrospec™ 3100 pro, Biochrom). The standard linear curve was established with a best fit to the measurement of 5 concentration standards (3.5, 7, 10.5, 14, 21 $\mu\text{g/ml}$) of bovine IgG. The optical density is only accurate up to a reading of 1.0. (i.e. where the standard curve remains linear.) In cases where the

absorption exceeded 1.0, the samples were diluted and measured again to ensure accurate results for the concentration of the proteins.

2.3.2.3. Dephosphorylation

One mechanism of posttranslational modification of the proteins involved in the circadian rhythm is phosphorylation and dephosphorylation (Schafmeier, Haase et al. 2005). In the circadian cycle, *frq*-RNA is translated into FRQ-protein and then subsequently phosphorylated, which seems to be an important step before degradation.

When performing gel electrophoresis and subsequent western blotting, this mechanism poses the problem that there might be two or more bands for the same protein – unphosphorylated and more or less phosphorylated protein. While two or more species of the same protein may give interesting insight into clock mechanisms, analysis of optical density of the total amount of protein is more accurate with single bands. Therefore some of the experiments, where two bands were visible on the film, were repeated after completely dephosphorylating the protein to consolidate the bands. These repeats with dephosphorylated protein were done as a proof of concept. Each dephosphorylated run showed the same results for total density as the previous phosphorylated run, assuring the accuracy of protein analysis. The data of these test Western blots is not shown.

For dephosphorylation 200 mg of extracted protein was mixed with dephosphorylation buffer and 10 U/ μ l of alkaline phosphatase (CIP – New England

BioLabs) to give a final volume of 50 μ l. This was incubated for 1 hour at 37°C. After incubation, gel electrophoresis, as described in 2.3.2.4, was performed.

2.3.2.4. Gel electrophoresis

I used SDS-polyacrylamide gel electrophoresis (SDS-PAGE). To prepare the gels, first the resolving gel was poured between two glass plates, divided by two spacers, creating a chamber (size: 9.5 cm x 14 cm x 0.2 cm). With a layer of isopropanol on top of the resolving gel to achieve a level surface, the gel was polymerized. 45 minutes later, the isopropanol was completely washed out, a stacking gel (size: 2.5cm x 14cm x 0.2cm) was poured on top of the resolving gel and a Teflon comb with 18 teeth introduced to create 18 wells for stacking. After placing the gel in the electrophoresis apparatus (custom made, Helmut Klausner, IMP workshop) and filling the anode and cathode chambers with running buffer, the wells were carefully cleaned from any excess gel and flushed with buffer several times.

Before loading the protein, 200 μ g of Protein was mixed with 1X Laemmle buffer and incubated at 95°C for denaturation. The protein was loaded onto the gel as well as 10 μ l of molecular weight standards (Precision Protein™ Standards, BioRad) and a negative control, consisting of a mutant with a knockout of the target gene chosen for that experiment. Electrophoresis was run at 80 V for about 90 minutes and changed to 125 V after the protein samples had reached the resolving

gel. The gel was then run for about 3 hours (depending on the target protein's size) until the dye front had exited the gel.

2.3.2.5. Western Blotting

For antibody probing, we blotted onto a nitrocellulose membrane. For electrophoretic transfer from the nitrocellulose membrane (PROTRAN®, Schleicher & Schuell) it was first wetted with Blotting buffer. The gel and the membrane were placed between two sheets of Whatman paper (GB 002 Gel-Blotting Paper, Schleicher & Schuell), also soaked with Blotting buffer. After carefully rolling out possible air-bubbles with a reagent tube, the sandwich was put into the blotting cassette between two thin sponges and then put into the blotting chamber (TransBlot™ Electrophoretic Transfer Cell, BioRad®), filled with blotting buffer. The transfer was run at 800 mA for two hours. After blotting, the membrane was rinsed with ddH₂O to remove the SDS and stained with Ponceau-S solution for 20 seconds to be able to inspect the blot. The excess Ponceau-S was rinsed away with ddH₂O and the membrane then left to air-dry over night.

For proteins smaller than 80-90 kD, another blotting chamber was used. The custom made (Helmut Klausner, IMP workshop) semi-dry blotting chamber contained two graphite electrodes. The blotting was driven by a constant current of 2 mA/cm² (of sandwich area). The transfer time was 90 minutes. After that the above described Ponceau staining was performed. (Towbin, Staehelin et al. 1979)

2.3.2.6. Probing for target proteins

The membrane was bathed and gently shaken in TBS Blotting buffer for 10 minutes to remove the Ponceau-S staining. To block the nitrocellulose membrane, it was incubated with 50 ml of 5% milk (skim milk powder in TBS, filtered before use) for one hour. The milk was poured off and 50 ml of milk with a 1:40 dilution of the primary antibody was added. With gentle shaking at room temperature for two hours the binding of antibody and protein was allowed. The primary antibody was poured off and the membrane washed with TBS to remove excess antibodies. The secondary antibody (in 5% milk, dilution 1:5000 for monoclonal primary antibody, 1:10 000 for polyclonal primary antibody), coupled to horse-radish-peroxidase, was incubated with the membrane for 12-20 hours at 4°C with gentle shaking. The next day the antibody-milk solution was poured off and the membrane washed with TBS three times and shaken in TBS for 15 minutes to remove unbound secondary antibodies.

Table 2.2: Antibodies used in this study

<u>Antibody</u>	<u>Antigen</u>	<u>Origin</u>
α -FRQ(3G11)	MPB-FRQ(65-989 aa) (Merrow, Franchi et al. 2001)	monoclonal, mouse
α -VVD	VVD-2 (13-29aa) (Michael Brunner, personal communication)	polyclonal, rabbit

2.3.2.7. Developing the membrane

The membrane was placed in a plastic envelope, and the excess TBS was carefully wiped out off the envelope. 2ml of Luminol solution (Lumi-Light^{Plus}®, Roche) was poured over the membrane. The excess Luminol was removed after 2 minutes. Then film (Medical X-ray film 100, Fuji) was exposed to the membrane for different amounts of time to achieve different staining density and then developed. (Airclean 200/35 plus - film developing machine, Protec, Germany)

2.3.2.8. Analysis of the developed film

All developed films were scanned (AGFA Snapscan 1236, settings: resolution 150 dpi, grayscale) and saved as .pict-files. The optical density of each band, correlating with the amount of target protein, was determined with the *Video analysis 1.8* program (Prof. T. Roenneberg, LMU Munich).

The density values for the different exposure times were transferred into the *Kaleidagraph 3.0.1.* program. There, they were fitted to a sigmoidal curve: $(y=m1*(((x+m3)/m2)/(1+((x+m3)/m2)^2)^{0.5})+m4)$, where y represents the pixel density and x the exposure time. This process gives more accurate quantifications over a larger dynamic range than using a single exposure.

3. Results

3.1. Physiological results

3.1.1. Skeleton photoperiods (SPP)

The experimental setup (see section 1.5) and the graphical method for evaluation (see section 2.2.2.2) of the skeleton photoperiods are described above. In short, the three strains of *Neurospora* with three different free running periods (frq^+ , frq^1 and frq^7) were exposed to 24 hour cycles with 2 light pulses of 2 hours length each, separated by different lengths of time. The systematic setup also included one cycle with a 4 hour light pulse (i.e. 2 light pulses with no dark pulse in between, i.e. 4 h light : 20 h dark) and also one cycle with only one 2 hour light pulse (2 light : 22 dark). Although all three strains were exposed to the same cycles, they yielded different but systematic results. They illustrated in figures 3.1 – 3.3, with only the onset of conidiation depicted in the respective graphs.

Skeleton photoperiods are an artificial approach to investigate circadian properties by mimicking a full photo period with two separate light pulses. But those two pulses can be seen as mimicking the non-parametric beginning and ending of a single light period. Therefore, while describing and analyzing the results from skeleton photoperiods, an assumption of which interval between light pulses is the “day” and which is the “night” has to be made. So first, the results from the frq^+ cycles will be described and the assumption of one of the intervals as the “day” will be used when describing the results from the frq^1 and frq^7 cycles.

1. In the frq^+ strain (figure 3.1.), *Neurospora* assumes a stable phase angle at the midpoint between the light pulses in each cycle. Because *Neurospora crassa* starts to band around midnight in full photoperiods, it can be assumed that the longer portion between the two skeleton photoperiods is interpreted as night. So, as in full photoperiods of $T = 24$ h, *Neurospora* entrains to midnight with its onset of conidiation (compare section 3.1.2 and previous experiments: Tan, Merrow et al. 2004) and the onset of conidiation is around midnight. This holds for all non-symmetrical cycles, where *Neurospora* shows only one conidial band per 24 hour cycle. In the symmetrical and near symmetrical cycles, *N.c.* shows two bands per 24 hour cycle and a distinction between a subjective night and day can not be made.

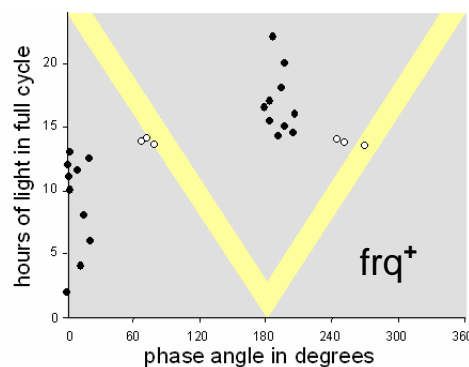


Figure 3.1: Phase angles of onset of conidiation in the skeleton photoperiods for the frq^+ strain. Filled circles denote cycles with one band every 24 hours, open circles denote cycles with two bands per 24 hour cycle. The yellow bars represent the two hour light pulses and are correct in their relative size.

Thus, the results of the frq^1 and frq^7 cycles can be described with the assumption that the longer interval is interpreted as the night in the skeleton photoperiods.

2. Unlike frq^+ , frq^1 entrains coupled to the dawn lights-on, and again shows a phase jump at around the symmetrical cycles. The onset of conidiation has a phase angle of about 180° (12 hours) after the dawn lights-on.
3. As frq^1 , frq^7 entrains coupled to the dawn lights-on signal in SPP cycles, again with a phase jump at around the symmetrical cycles. Unlike in frq^1 , the onset of conidiation in frq^7 lags dawn by 22-23 hours.

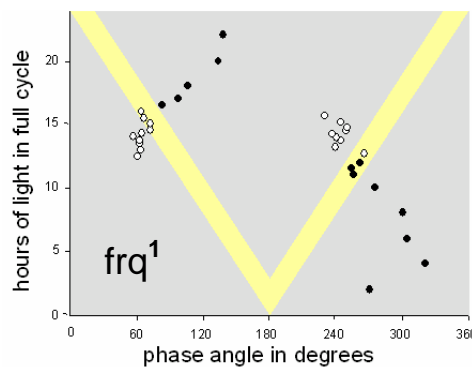


Figure 3.2: Phase angles of onset of conidiation in the skeleton photo periods for the frq^1 strain. Filled circles denote cycles with one band every 24 hours, open circles denote cycles with two bands per 24 hour cycle. The yellow bars represent the two hour light pulses and are correct in their relative size.

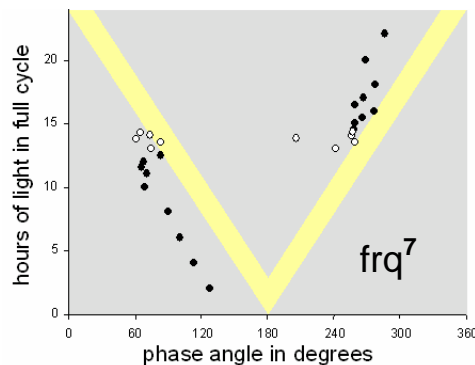


Figure 3.3: Phase angles of onset of conidiation in the skeleton photo periods for the frq^7 strain. Filled circles denote cycles with one band every 24 hours, open circles denote cycles with two bands per 24 hour cycle. The yellow bars represent the two hour light pulses and are correct in their relative size.

One of the major questions of this thesis is, whether *Neurospora* is driven or entrained by light cycles. As shown above, the coupling of the phase angle to

midnight in the *frq⁺* strain already shows entrainment, but also the phase jump around the symmetrical cycles cannot be explained with drivenness. When expecting drivenness, a strain should take a phase angle to one light pulse and not exhibit a jump. Drivenness would give a uniform reaction to a stimulus. And also in these experiments, an irradiance effect does not explain the data, as the cycles all have a total of 4 hours of light (with the 2 h light: 22 h dark as an exception). Thus, *Neurospora* entrains to skeleton photo periods, rather than being driven by them.

3.1.2. The circadian surface

The only experiment that had used the term “circadian surface” previously was a study, where the induction of diapause (resting state) of a beetle was investigated under varying lengths of symmetrical light-dark cycles (Beck 1962). We chose the term “circadian surface”, because it very well illustrates the experimental approach. Three variables were changed in assembling the circadian surface: (1) the length of the T-cycles, (2) the amount of light per T-cycle and (3) the free-running period of the studied strains (see section 1.5 for more details). The T-cycles ranged from 16 hours to 26 hours (16 h, 18 h, 20 h, 22 h, 24 h and 26 h), the light amounts ranged from 16% to 84% (16%, 25%, 33%, 40%, 50%, 60%, 67%, 75% and 84%). This results in 54 experimental conditions for each of the three strains (*frq⁺*, *frq¹* and *frq⁷*). For each strain and condition 6-12 race tubes were used. To verify results, each condition was repeated at least twice with 3-12 race tubes. The results are shown in figures 3.4 through 3.21, sorted by strains and T-cycle length.

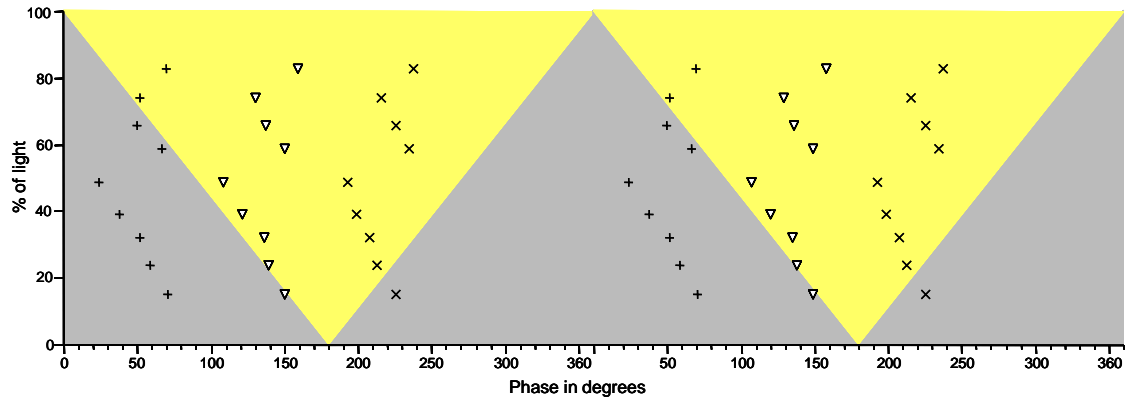


Figure 3.4.: conidiation (+ = onset, Δ = peak, x = offset of conidiation) in the 16h T-cycle for the *frq*⁺ strain.

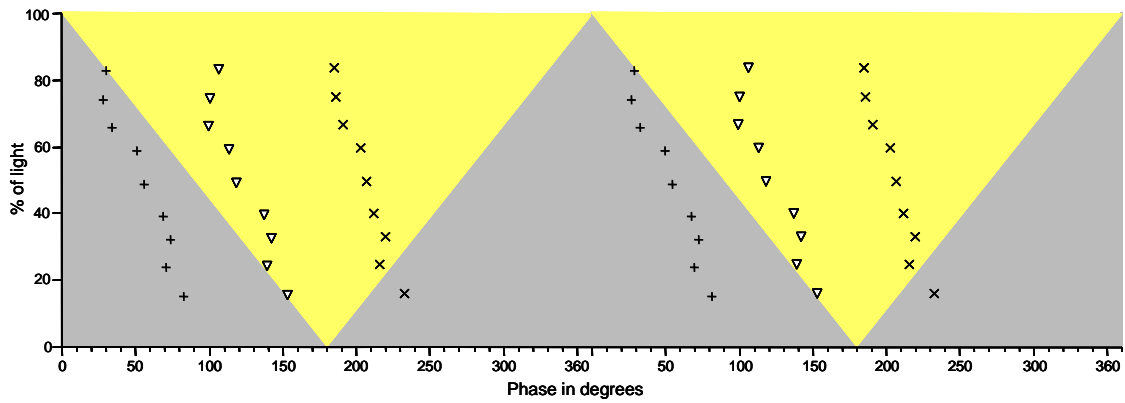


Figure 3.5.: conidiation (+ = onset, Δ = peak, x = offset of conidiation) in the 18h T-cycle for the *frq*⁺ strain

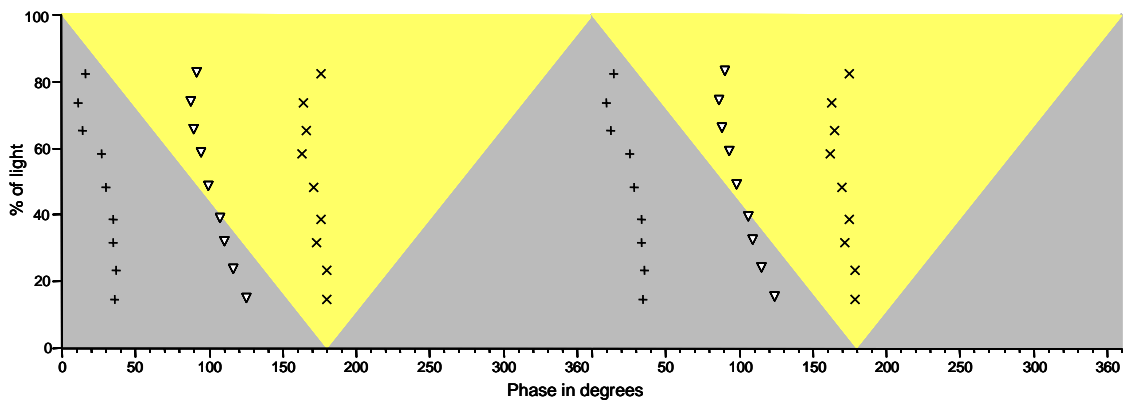


Figure 3.6.: conidiation (+ = onset, Δ = peak, x = offset of conidiation) in the 20h T-cycle for the *frq*⁺ strain

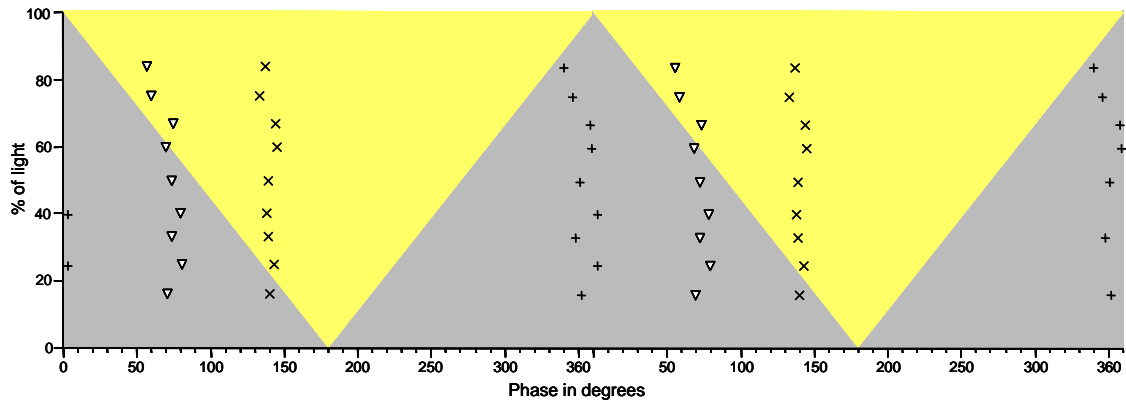


Figure 3.7.: conidiation (+ = onset, Δ = peak, x = offset of conidiation) in the 22h T-cycle for the *frq*⁺ strain

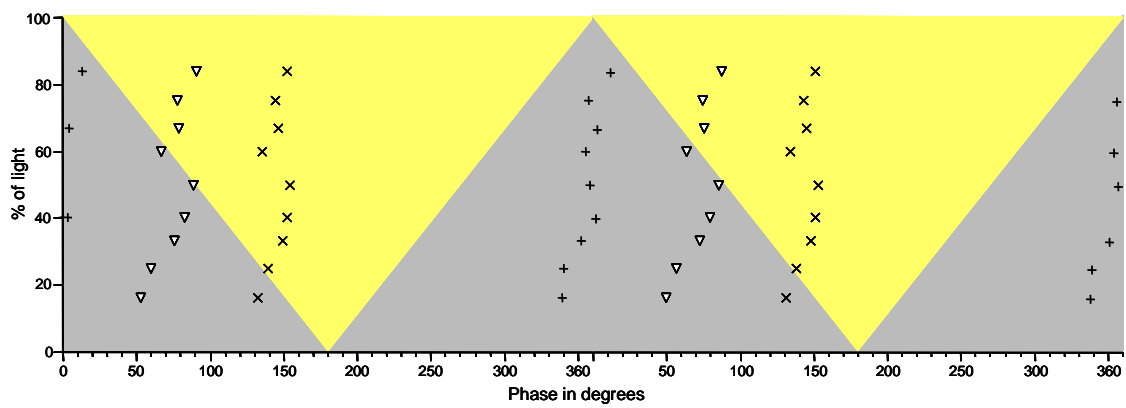


Figure 3.8: conidiation (+ = onset, Δ = peak, x = offset of conidiation) in the 24h T-cycle for the *frq*⁺ strain

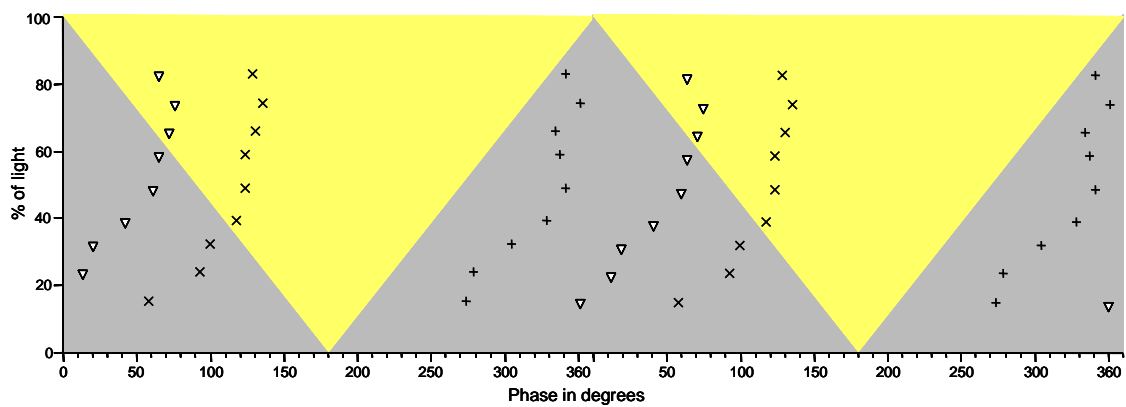


Figure 3.9.: conidiation (+ = onset, Δ = peak, x = offset of conidiation) in the 26h T-cycle for the *frq*⁺ strain

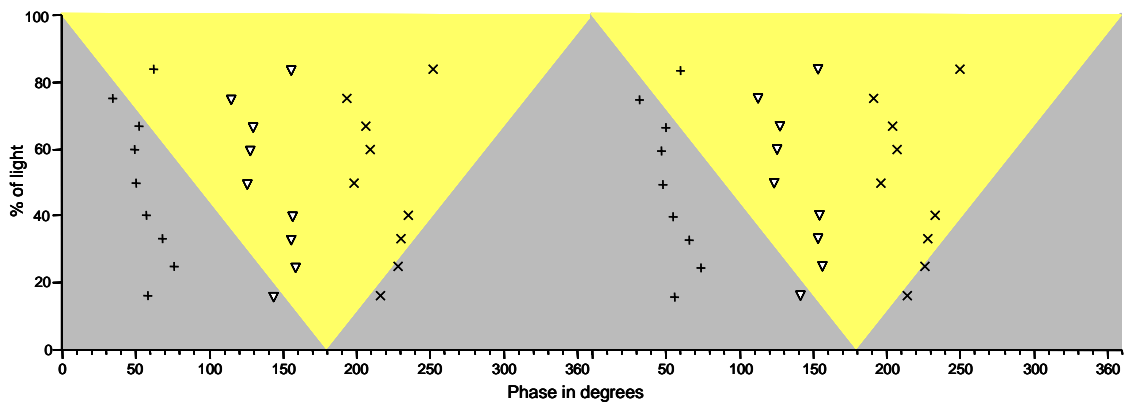


Figure 3.10.: conidiation (+ = onset, Δ = peak, x = offset of conidiation) in the 16h T-cycle for the *frq1* strain

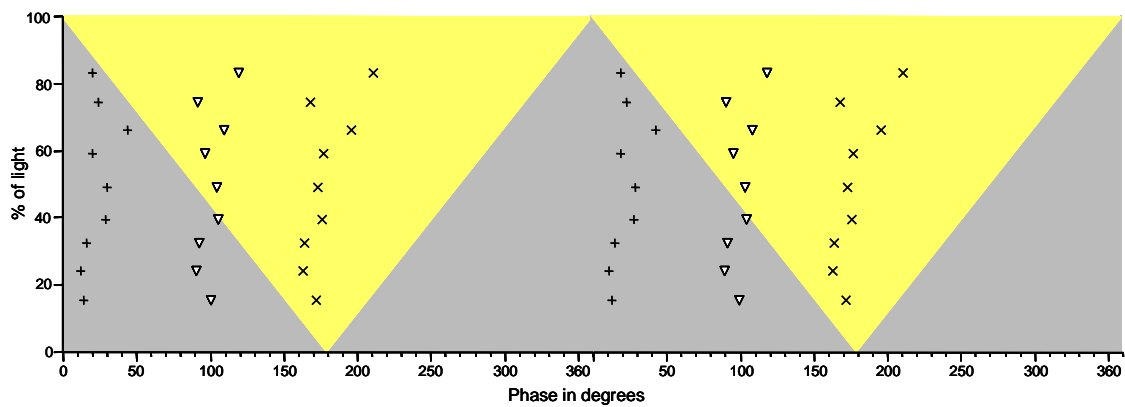


Figure 3.11.: conidiation (+ = onset, Δ = peak, x = offset of conidiation) in the 18h T-cycle for the *frq1* strain

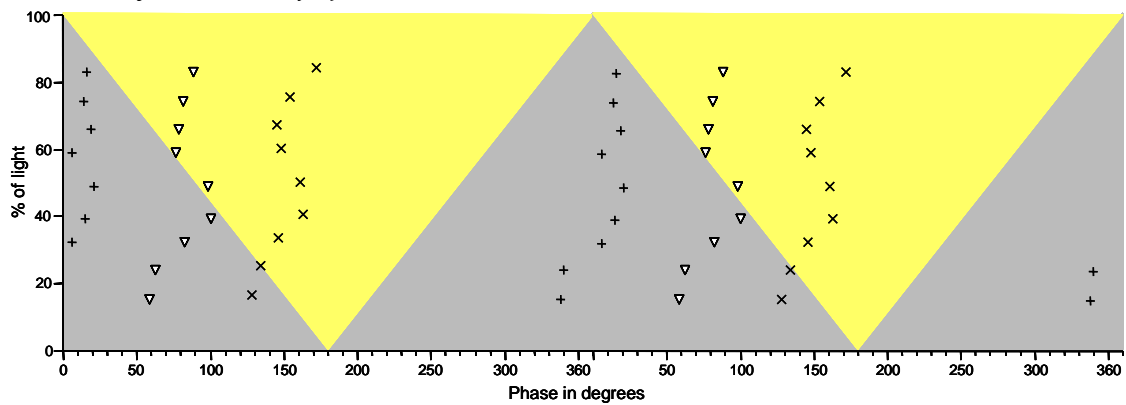


Figure 3.12.: conidiation (+ = onset, Δ = peak, x = offset of conidiation) in the 20h T-cycle for the *frq1* strain

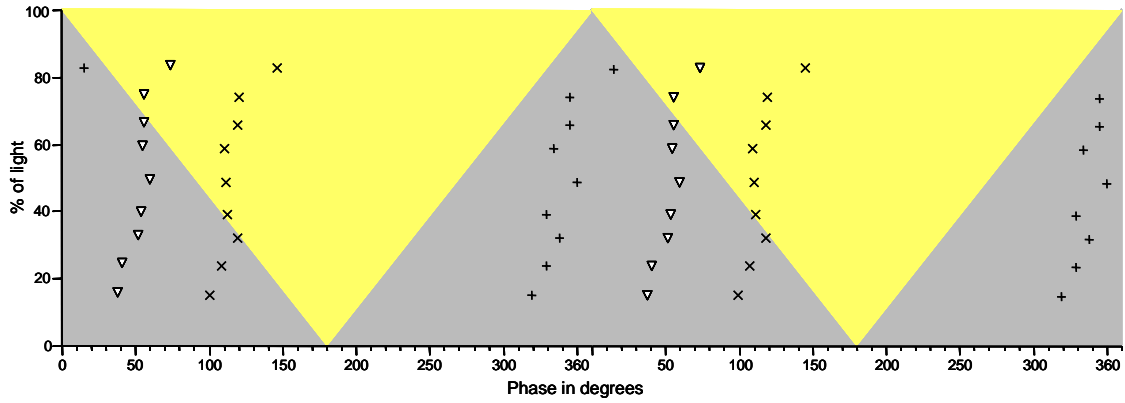


Figure 3.13.: conidiation (+ = onset, Δ = peak, x = offset of conidiation) in the 22h T-cycle for the *frq1* strain

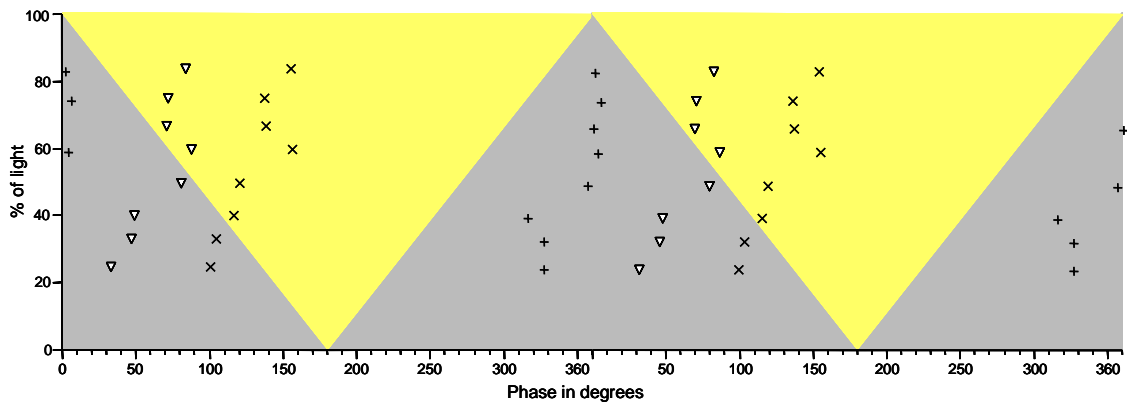


Figure 3.14.: conidiation (+ = onset, Δ = peak, x = offset of conidiation) in the 24h T-cycle for the *frq1* strain

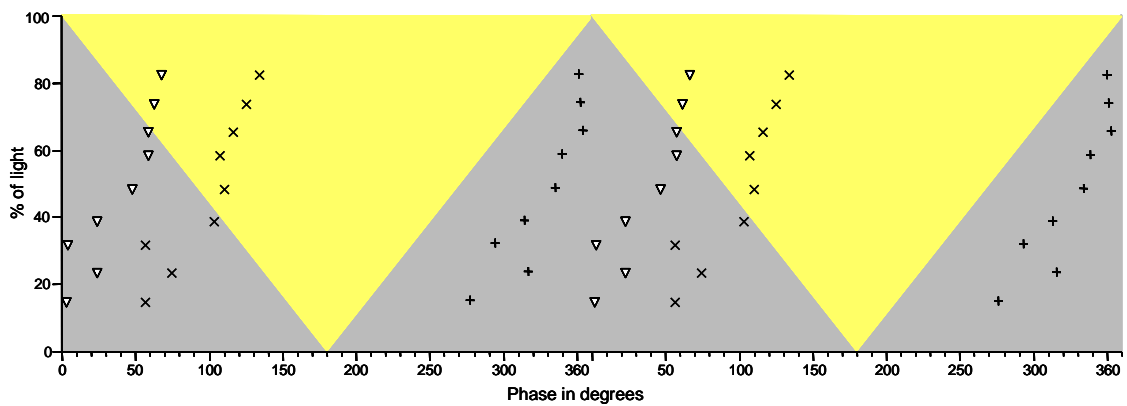


Figure 3.15.: conidiation (+ = onset, Δ = peak, x = offset of conidiation) in the 26h T-cycle for the *frq1* strain

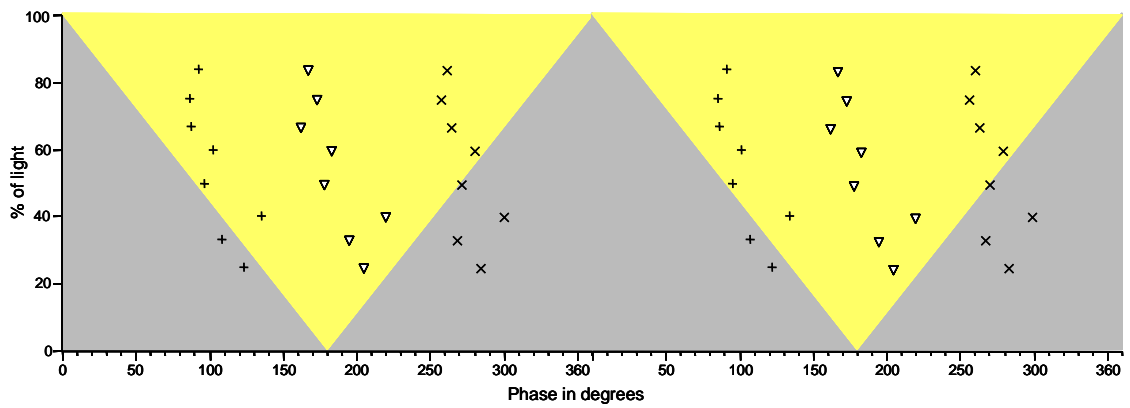


Figure 3.16.: conidiation (+ = onset, Δ = peak, x = offset of conidiation) in the 16h T-cycle for the *frq7* strain

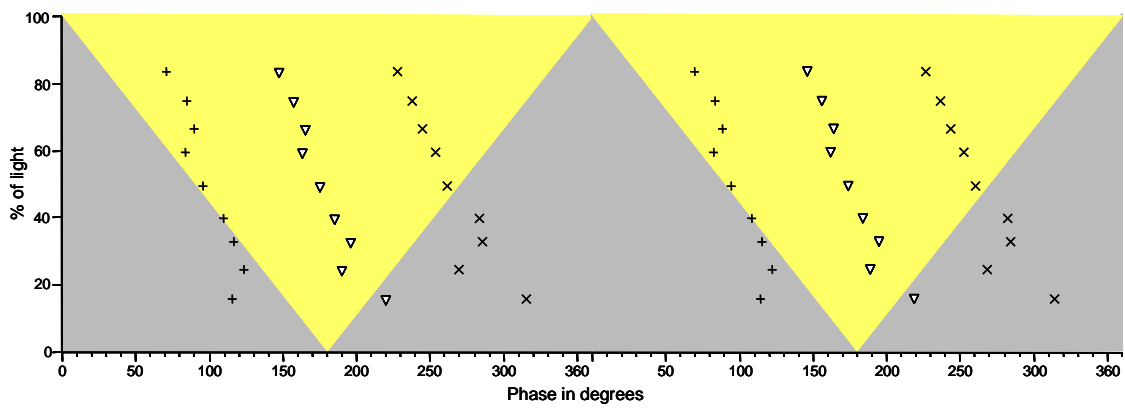


Figure 3.17.: conidiation (+ = onset, Δ = peak, x = offset of conidiation) in the 18h T-cycle for the *frq7* strain

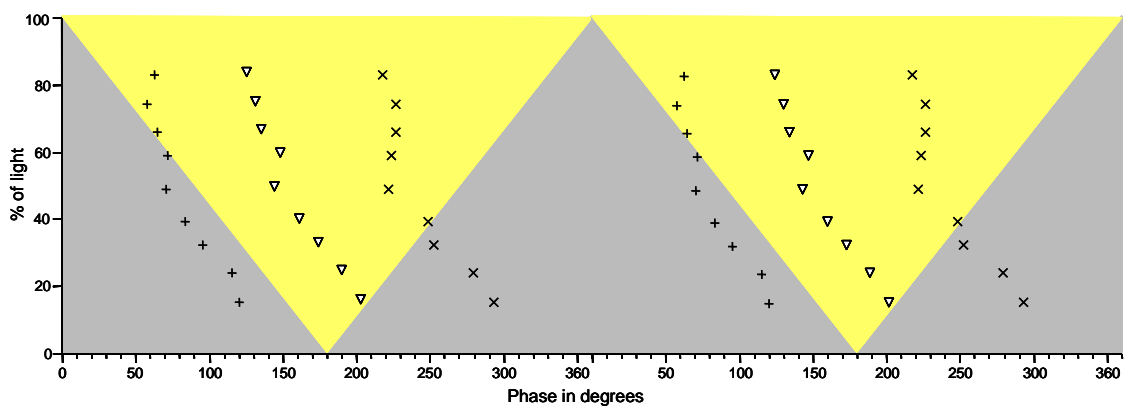


Figure 3.18.: conidiation (+ = onset, Δ = peak, x = offset of conidiation) in the 20h T-cycle for the *frq7* strain

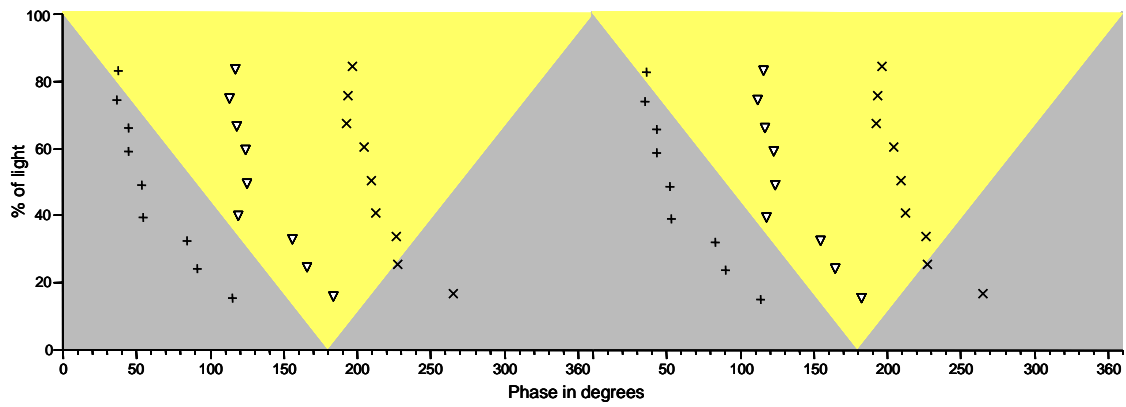


Figure 3.19.: conidiation (+ = onset, Δ = peak, x = offset of conidiation) in the 22h T-cycle for the *frq7* strain

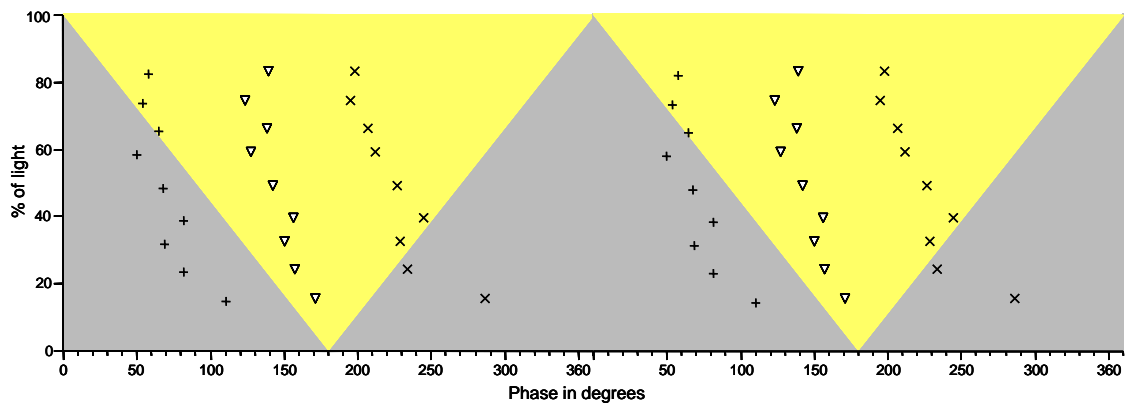


Figure 3.20.: conidiation (+ = onset, Δ = peak, x = offset of conidiation) in the 24h T-cycle for the *frq7* strain

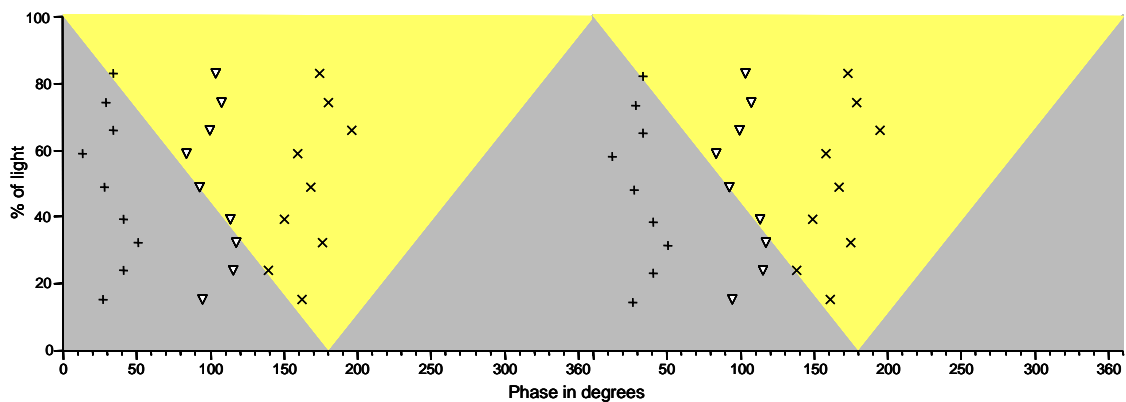


Figure 3.21.: conidiation (+ = onset, Δ = peak, x = offset of conidiation) in the 26h T-cycle for the *frq7* strain

The results add up to a highly systematic but simple set of rules for entrainment to light cycles:

A. Long photoperiods (more than 50% of light per cycle):

1. *Neurospora crassa* entrains with coupling to midnight.
2. The longer T (cycle length) in relation to the τ (= FRP, free running period), the more conidiation is delayed in relation to midnight.

B. Short photoperiods (less than 50% of light per cycle):

1. If $T < \tau$, *N.c.* couples to dawn.
2. If $T > \tau$, *N.c.* couples towards dusk.
3. If $T = \tau$, *N.c.* couples to midnight.

3.2. Molecular results

3.2.1. Choosing cycles for molecular analysis

Evaluation of the circadian surface revealed three 'types' of entrainment: phase coupled (or "locked") to dawn, to dusk or to midnight. Clock gene expression was investigated in one case of each of these entrainment phenotypes.

Three cycles were chosen to be tested with the *frq*⁺-strain for molecular analysis: T16 (LD 4:12), T22 (LD 4:18) and T26 (LD 4:22). Cycles with equal absolute duration of the light phase were specifically chosen, so that irradiance effects could be excluded. The *frq*⁺-strain has a free running period (τ) of about 22 h and therefore with the three cycles, 3 different relationships of T and τ are tested for their molecular profile:

1. In T = 16 (T < τ), the conidiation phase angles of *Neurospora crassa* are locked to dawn, i.e. the phase angle in the shorter photoperiods (below 50% light) is parallel to the dawn dark-light transition (fig. 3.22).
2. In T = 22 (T = τ), the conidiation phase angles of *Neurospora crassa* are locked to midnight (fig. 3.22).
3. In T = 26 (T > τ), the conidiation phase angles of *Neurospora crassa* are locked to dusk (fig. 3.22).

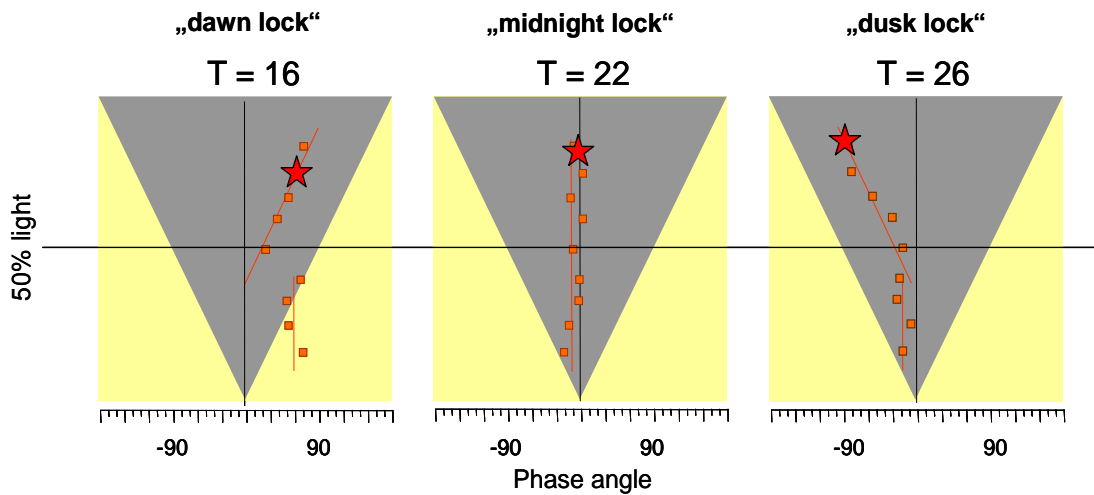


Figure 3.22.: The three graphs for the T16, T22 and T26 cycles show the phase angles of the onset of conidiation in the $freq^+$ strain of *Neurospora crassa*. For orientation, the slopes of the phase angles are fitted with lines. The cycles that were chosen for molecular analysis are pointed out with stars. (Compare with graphs in section 3.1.)

3.2.2. RT-PCR results

The results of the mRNA analysis using RT-PCR (figs. 3.23 – 3.27) reproduce and extend previous results (Tan, Dragovic et al. 2004). *freq*-mRNA is rapidly upregulated, reaching its highest level in each cycle at the 15 minute timepoint. This is similar to the results of Crosthwaite (1995). The Crosthwaite study could also show that *freq*-levels remained elevated when lights were kept on. With the longer light-stimulus in this study (4 hours vs. a 2 minute light pulse in Crosthwaite's study), both elements are shown: the levels of *freq*-mRNA rise quickly after lights on, remain elevated during the light and start decreasing right after lights-off. In our group's previous studies, we noted a non-systematic relationship between RNA and protein (discussed below), but the results for mRNA were comparable despite the different

structure of the cycles (Tan, Dragovic et al. 2004). The one difference in RNA results between the different cycles with different length is, how long the levels of *frq* remain elevated. Namely, the longer the cycle, the longer the levels are elevated above baseline (level before lights on). Specifically, the *frq*-levels reach baseline after about 8.5 hours in T=16, after about 10 hours in T=22 and after about 13.5 hours in T=26. (See figs. 3.23 – 3.25, sorted by strains)

The *vvd*-mRNA is also acutely induced by lights-on. Comparing the levels before and 15 to 30 minute after lights on, the levels increase about 50 times in T=16 and T=26, and about 20 times in the T=22. The kinetics for up-regulation are similar in all cycles, and the down-regulation starts in all cycles right after the early peak. But, similar to *frq*-levels, the cycles differ in the duration of elevated levels of mRNA. Specifically, the *vvd*-levels reach baseline (level before lights on) after about 8.5 hours in T=16, after about 10 hours in T=22 and after about 13.5 hours in T=26 (See figs. 3.23 – 3.25, sorted by strains). Although we do not yet understand the mechanism, it is worth noting that the regulation of the post-light induced levels of these two different RNAs is highly similar.

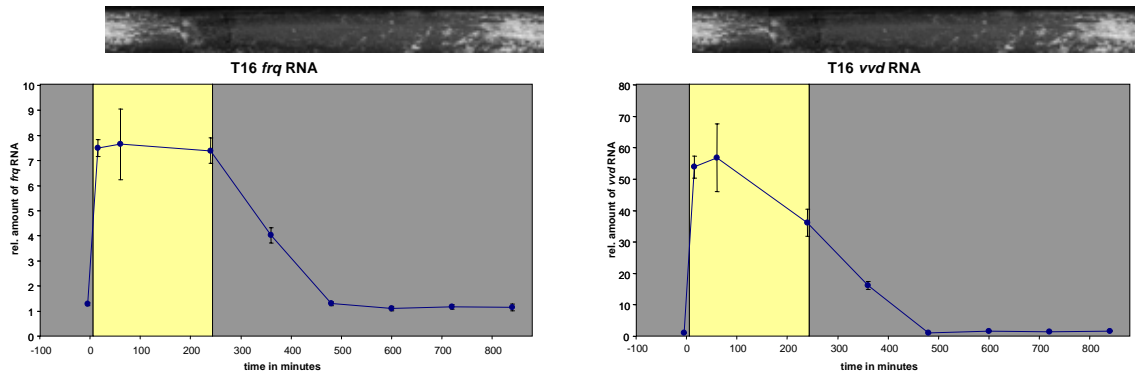


Figure 3.23: The results of the RT-PCR for the T16 cycle are plotted with relative amount against time. The left graph showing *frq* RNA levels and the right graph showing the *vvd* RNA levels. The light cycle is plotted as the background of the graph, with yellow corresponding to the photoperiod and gray corresponding to the scotoperiod. The image above the graph represents the phase position of the conidial band.

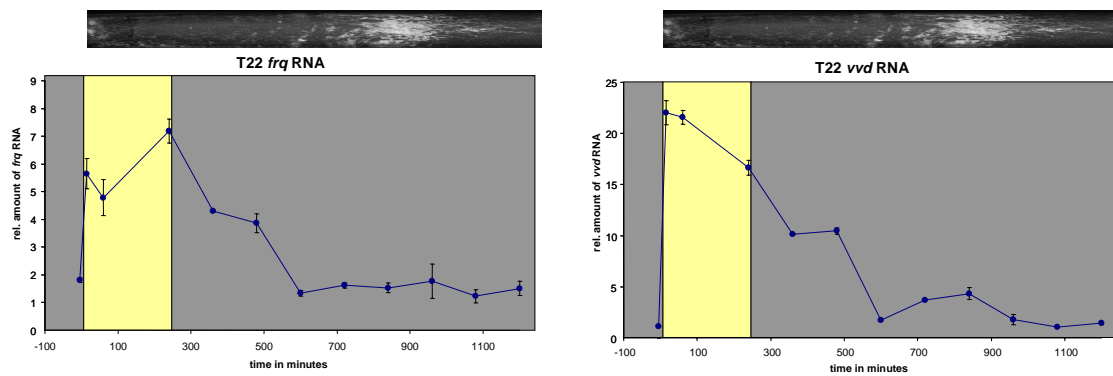


Figure 3.24: The results of the rtPCR for the T22 cycle are plotted with relative amount against time. The left graph showing *frq* RNA levels and the right graph showing the *vvd* RNA levels. See fig. 3.23 for further explanation.

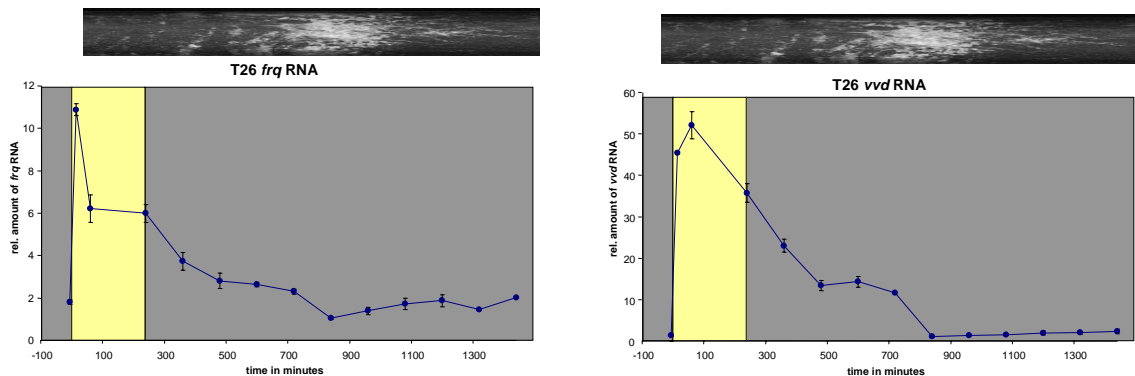


Figure 3.25: The results of the rtPCR for the T26 cycle are plotted with relative amount against time. The left graph showing *frq* RNA levels and the right graph showing the *vvd* RNA levels. See fig. 3.23 for further explanation.

wc-1 mRNA remains level at about 2 relative units throughout each cycle, but is quickly up-regulated by light, reaching its highest amplitude in each cycle at the 15 minute time point. Comparing the three cycles, the difference is in the amplitude of the acute RNA peak. It is highest in T=26 and lowest in T=22.

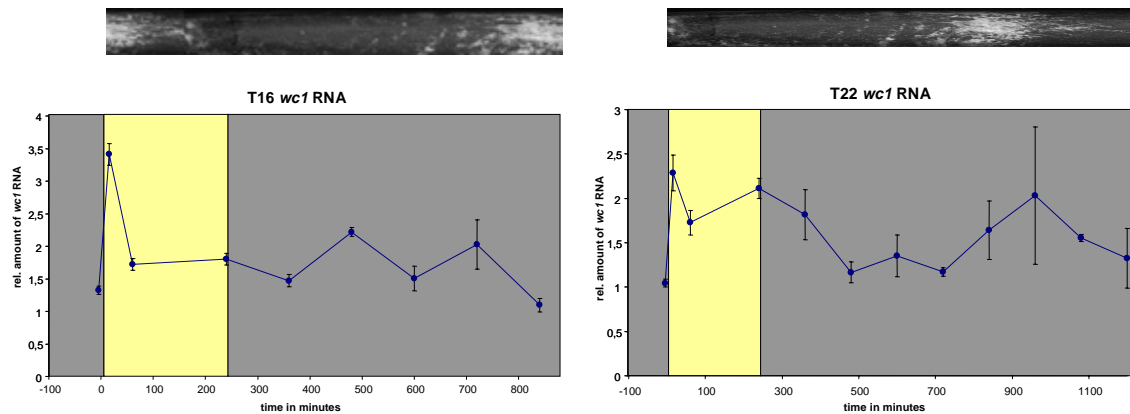


Figure 3.26: The results of the rtPCR for *wc-1* RNA levels in the T=16h and T=22h cycles are plotted with relative amount against time. The left graph shows the T=16 cycle, the right graph the T=22 cycle. See fig. 3.23 for further explanation.

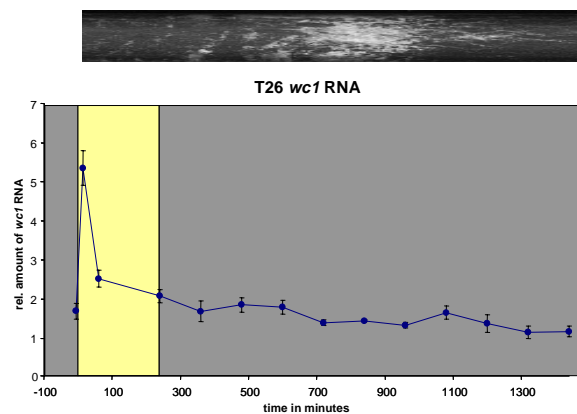


Figure 3.27: The results of the rtPCR for *wc-1* RNA levels in the T=26 cycle. See fig. 3.23 for further explanation.

3.2.3. Western blot results

Given our previous results, showing dissociation of *frq* RNA and protein in entrained conditions, I investigated expression of FRQ and VVD protein (see section 1.4. for description of function and interaction). As to be expected, there is a lag between the peak of RNA (see section 3.2.2) and protein levels (fig. 3.28). The signature transition from unphosphorylated (early in the cycle) to phosphorylated FRQ protein (later in the cycle) is also seen in all three T-cycles. Also similar to previous results (Tan, Dragovic et al. 2004), the onset of conidiation occurs following the peak of FRQ protein, although in this case conidiation occurs slightly earlier, relative to the disappearance of FRQ. The peak of protein levels is approximately the same in all cycles, about 8.5 hours after lights on. The cycles differ in the degradation of FRQ, with the levels of FRQ staying elevated until shortly before the next lights-on transition. Also note that in T = 16 h and T = 22 h there is an initial decrease of FRQ levels following lights on. Previously, only increases in FRQ levels have been invoked to explain entrainment. It may be that degradation is important for entrainment also.

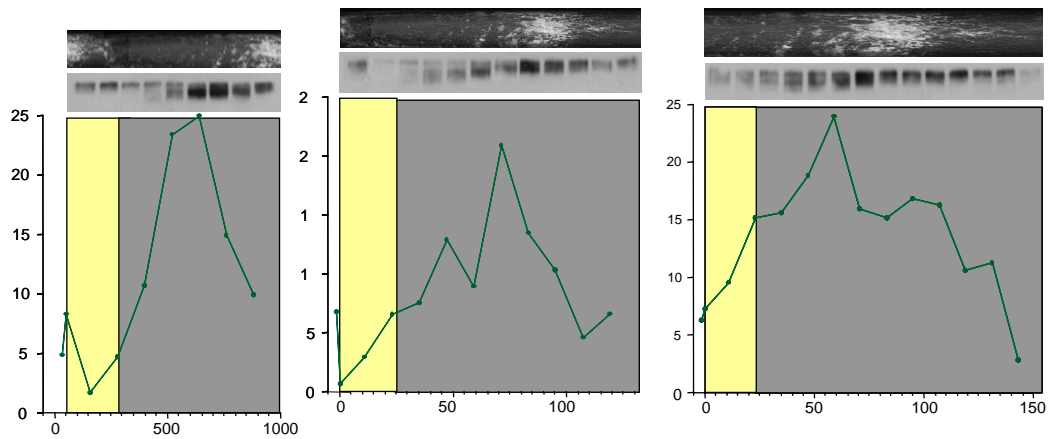


Figure 3.28.: The graphs show the relative amount of FRQ-protein over the course of the respective cycle (T16 right, T22 middle, T26 left). The x-axis shows time in minutes, the y-axis shows relative amounts. The pictures above the graphs show the original developed x-ray film and a representation of the conidiation in the respective cycles. Please note that the gel-lanes are not aligned with the respective data points on the graph, as they more densely timed around lights-on.

I also probed Western blots for the VVD-protein. These blots represent the first ever reported for VVD in a LD cycle. The blots show that production of VVD is rapid in all cycles. Soon after lights on, VVD levels rise and reach their maximum at lights off, 4 hours after lights on. The one marked difference in the three cycles and their VVD-kinetics is the degradation. Where the peaks are alike in all cycles, degradation changes systematically with the length of the cycle. In all cycles, the degradation takes the whole scotoperiod to be complete. Namely 12 h in the T = 16 h, 18 h in the T = 22 h and 22 h in the T = 26 h cycle. The degradation of VVD is linear from peak to baseline levels (the levels before lights on) and, therefore, fails to correlate with either FRQ levels or with *vvd*-RNA. In up-regulation, protein correlates with the RNA-kinetics (compare figs. 3.23 - 3.25 and 3.29).

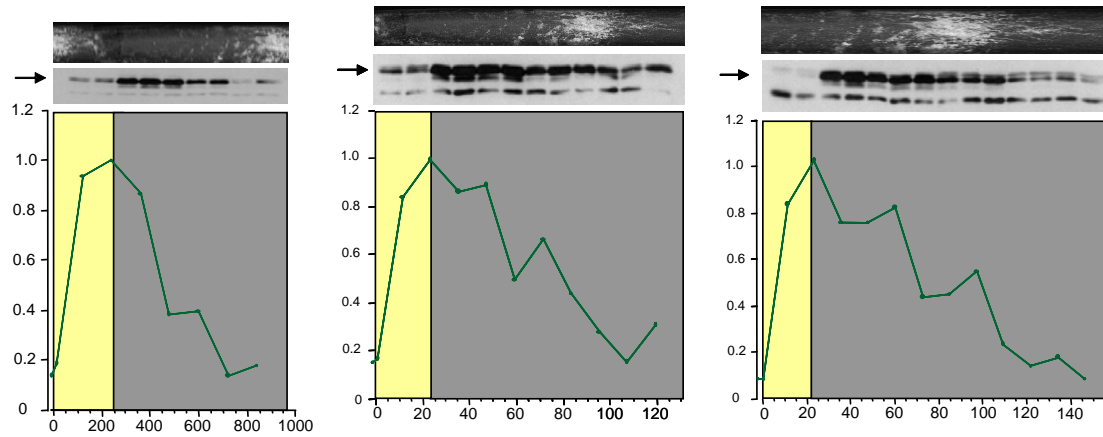


Figure 3.29.: The graphs show the relative amount of VVD-protein over the course of the respective cycle (T=16h right, T=22h middle, T=26h left). The x-axis shows time in minutes, the y-axis shows relative amounts. The pictures above the graphs show the original stained x-ray film and a representation of the conidiation in the respective cycles. The arrows indicate the VVD-band on the gel. Please note, that the gel-lanes are not aligned with the respective data points on the graph, as they are more densely timed around lights-on.

4. Discussion

As described above (see section 1.2.), a circadian system has several defining properties: rhythmicity, a circadian range, a large enough amplitude and sustainability of the output rhythm, noise compensation and entrainability. With this thesis mainly one of the circadian properties of the model organism *Neurospora crassa* has been investigated: entrainment on the physiological and on the molecular level.

The physiology and molecular biology of entrainment has been investigated in many organisms (Bruce 1960; Crosthwaite et al. 1995; Merrow et al. 1999) and rules for entrainment have been deduced (Roenneberg, Daan et al. 2003). Yet entrainment has by far not been studied as systematically in such a wide spectrum of conditions in a single organism as in this thesis.

4.1. *Neurospora crassa*'s behavior in light-dark cycles

In *N. crassa*, entrainment to temperature cycles and to a limited number of light cycles has been demonstrated on the physiological level (Merrow, Brunner et al. 1999; Tan, Merrow et al. 2004). In other studies that adressed light responses (Crosthwaite, Loros et al. 1995; Crosthwaite, Dunlap et al. 1997; Liu 2003), the reaction to single light pulses was examined and showed a distinct phase change (onset of conidiation in following cycle) with those light pulses. (The corresponding molecular results will be addressed in section 4.2.)

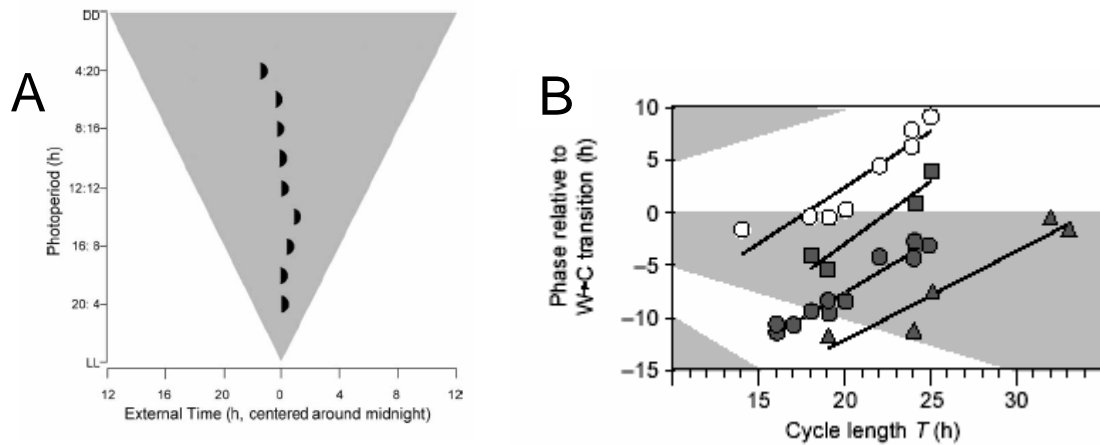


Figure 4.1: **A)** Phase angles of conidiation for *N.crassa* in different photoperiods within a 24 h cycle, showing photoperiodism. (Tan, Merrow et al. 2004) Note that the phase is coupled to midnight. **B)** Phase angles of conidiation for three different *N. crassa* mutants in symmetrical temperature cycles. The three mutants: *frq⁺*, *frq¹* and *frq⁷* differ in their free running period (see graph). The lines are fitted curves (Merrow, Brunner et al. 1999).

These phase changes with one-time light exposure, or repeated zeitgeber exposures in general, have also been demonstrated in other organisms. They showed that entrainment is a dynamic process of synchronization that can take days to reach a stable state and, therefore, experiments where the reaction to single light signal are recorded will show how the clock reacts to that single light signal (mostly with a discrete change of phase), but may fail to accurately capture the dynamic mechanisms of entrainment. This thesis is the first to systematically show entrainment to full photoperiods as well as skeleton photoperiods.

4.1.1. Entrainment to skeleton photo periods

The results from the skeleton photo periods are summarized in figure 4.2. As described above (section 3.1.1), the two light portions seem to be computed as the beginning and the end of a single light period. Under these conditions, *Neurospora* (as other organisms) always chooses the longer interval as the night. The frq^+ strain entrains with the onset of conidiation coupled to midnight. The frq^1 and the frq^7 strains both entrain to dawn, but 180° out of phase from each other. The lag in the time of conidiation for the frq^1 and the frq^7 strain is the same as in the full photoperiods (about 11-12 hours), where frq^1 conidiates during the night and frq^7 during the day. So, the results from the skeleton photoperiods are compatible with earlier studies, and the frq^+ strain of *Neurospora* behaves as if the two pulses are computed as the non-parametric beginning and end of a full photoperiod (compare fig. 3.1 and fig. 3.8). This is also true for frq^7 (compare figs. 3.3 and 3.20), where the phase angle and its coupling to the dark-light transition is the same in skeleton photoperiods (SPPs) as in full photoperiods.

Only frq^1 does not show the same phase angle in SPPs as full photoperiods (compare figs. 3.2 and 3.14). This might be because the free running period (FRP) of frq^1 (16 h) is much shorter than the cycle length (24 h), allowing a full circadian oscillation in between the light periods. A coupling of the phase angle of the onset of conidiation to dawn is observed in T-cycles where $T < FRP$ (see fig 4.5). This allows to conclude that the frq^1 strain may not compute the two light periods per 24 hours as

the beginning and end of a single light period, most likely due to the short endogenous cycle compared to the longer dark period between two light signals. With the short FRP, *frq¹* can form 2 conidial bands per full 24 hour cycle, and 2 bands are actually observed in every strain around the symmetrical cycles (see figs 3.1 – 3.3), but the duration of the shorter of two dark periods is most likely not long enough to allow an additional conidial band. The length is always less than 10 hours, and only one band is seen when one of the dark periods is shorter than 9 hours. That actual time between the two light periods in the non-symmetrical cycles is most likely too short to allow an extra band, for example the 4 hours of darkness in a 2 hour light, 16 h dark, 2 h light and 4 h dark cycle.

Another explanation would be, that the mutation of the *frequency* gene in the *frq¹* strain does not result only in a shortened free-running period, but also that the mechanics of entrainment, namely the interaction with other proteins such as the white-collar complex is altered. This is seen in the entrainment to long full photoperiods (see fig. 4.7). If the mutation that results in a shortened free-running period would result in a linear change of phase of entrainment, the phase angles of entrainment in *frq¹* would extend the line that is drawn through the phase angles of *frq⁺* and *frq⁷*. *frq¹* does entrain with delays, as to be expected from a system with a short FRP, but with less of a lead with respect to midnight than to be expected from a linear change in entrainment behavior.

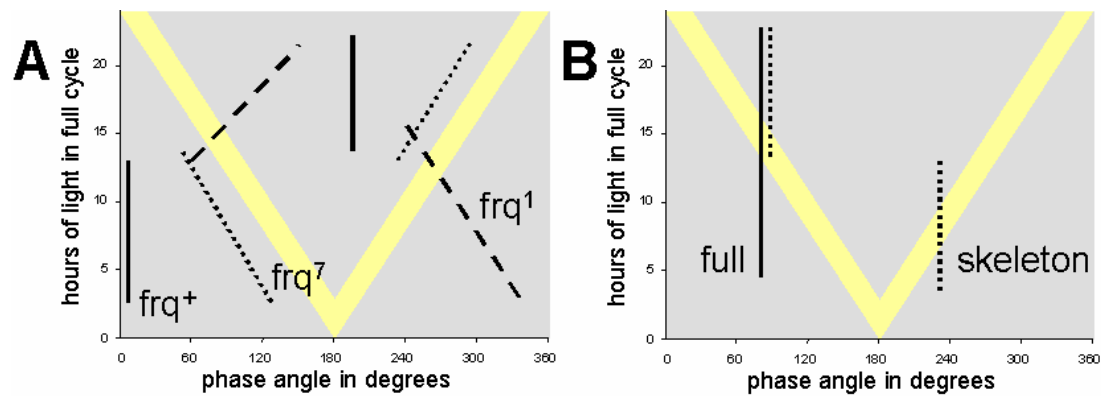


Figure 4.2: **A)** phase angles of conidiation for *N. crassa* in the skeleton photoperiods. The three different strains (solid line: *frq⁺*, dashed line: *frq¹* and dotted line: *frq⁷*) are shown with their onset of conidiation only. The yellow bars represent the two hour light pulses and are correct in their relative size. **B)** Eclosion rhythm of *Drosophila pseudoobscura* in full (solid line) and skeleton photo periods (dashed line). For the full photoperiods, the yellow bars represent the beginning (left bar) and the end (right bar) of the respective photoperiod. For the skeleton photoperiods, the bars represent a 15 minute light pulse each (widened from actual size). In full photoperiods, the eclosion rhythm is coupled to midnight and starts around dawn. In the skeleton photoperiod cycles, the rhythm is also coupled to midnight, but “phase jumps” at the 13h light : 11h dark cycle experiment. (Adapted from: Pittendrigh 1960)

With these results, the skeleton photo periods reveal complex mechanisms of entrainment, but are similar to what is seen in other organisms, with clear entrainment and a phase jump around the symmetrical skeleton photoperiods. Classical examples are the experiments by Pittendrigh (1960), where the same behavior (although 180° out of phase, with the activity period during the day, as *Drosophila* is a day active insect) was shown. In figure 4.2B these results are depicted, including the phase jump when the cycles become symmetrical. They show that *Neurospora* plays by the basic rules of entrainment (Roenneberg, Daan et al. 2003), and enables transfer of these results to other organisms, making the use of this model organism even more useful.

4.1.2. Entrainment on a circadian surface

The term “circadian surface” has been rarely used, as mentioned above (section 1.5 and section 3.1.2). The one study explicitly using it, studied seasonal behavior in insects (Beck 1962). Beck could show that insects adapt their diurnal behavior to the change of the seasons, a behavior called photoperiodism. That study and other studies showed that photoperiodism is not only observed in the context of a 24 hour day, but that also non-24 hour cycles can induce the physiological changes that characterize seasonal behavior, for example testis size in hamsters (Goldman 1999, Goldman 2001) or sporulation rhythm and carotenoid production in *Neurospora crassa* (Tan, Merrow et al. 2004).

This thesis builds in part on the previous photoperiodism studies, because photoperiodism and entrainment are closely linked by sharing circadian mechanisms. This was illustrated by observing the effect of mutations on circadian behavior that also changed photoperiodic behavior (Loudon, Ihara et al. 1998; Somers, Devlin et al. 1998). Our group expanded that approach to *Neurospora crassa* (Tan, Dragovic et al. 2004; Tan, Merrow et al. 2004).

To enhance these previous findings, this thesis systematically altered the experimental conditions to yield a circadian surface; covering 'all' cycle lengths and proportions of light. The results from the surface experiments lead to a systematic set of rules, listed in section 3.1.2. These results are summed up in figures 4.5 and 4.6 (please see section 3.1.2 for further details) and analyzed graphically in figure 4.7.

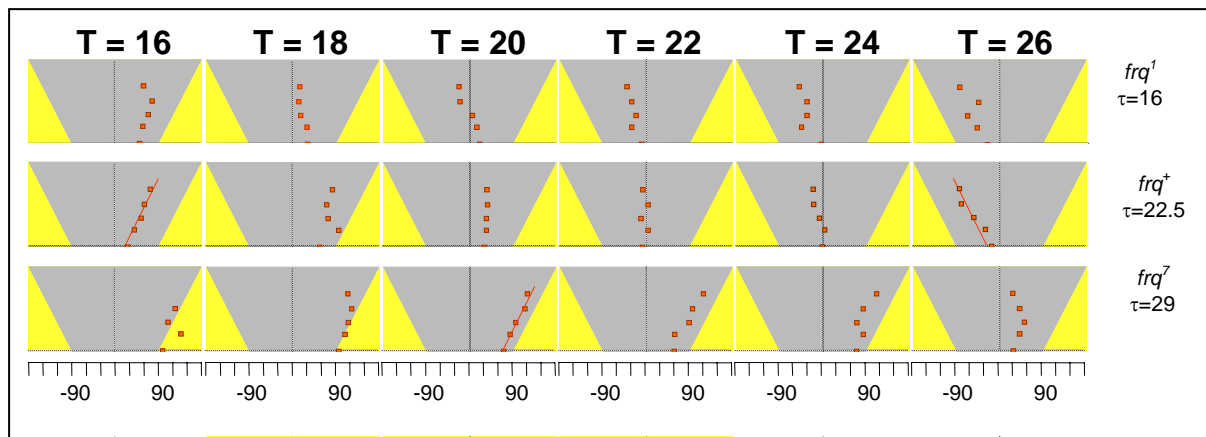


Figure 4.5: Results of the circadian surface for short photoperiods (< 50% of light per cycle). Shown are only the onsets of conidiation, being coupled to dawn, dusk or midnight. See section 3.1.2 for more details. The y-axis sorts the experiments by the proportion of light per cycle, the x-axis shows time in degrees ($360^\circ =$ one full cycle). (Graphs by Prof. Roenneberg)

In the long photoperiods (Fig. 4.7.A), where the phase angle is always coupled to midnight, the phase angle is the more advanced, the longer the cycle is. In 4.7.B, the results for short photoperiods show a change of the slope of the fitted lines. When T is short enough compared to τ (= FRP, free-running period), the phase angle of onset of conidiation is coupled to dawn. When T is long enough compared to τ , the phase angle of onset of conidiation is coupled to dusk. When T is approximately equal to τ , the phase angle is coupled to midnight.

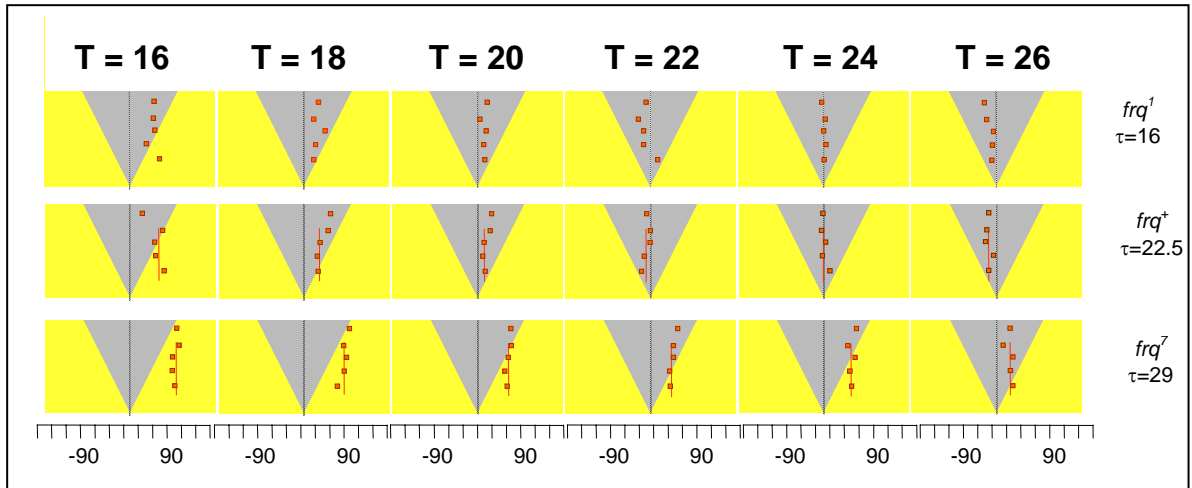


Figure 4.5: Results of the circadian surface for long photoperiods ($> 50\%$ of light per cycle). Shown are only the onsets of conidiation, which are coupled to midnight. See section 3.1.2 for more details. The y-axis sorts the experiments by the proportion of light per cycle, the x-axis shows time in degrees ($360^\circ =$ one full cycle). (Graphs by Prof. Roenneberg)

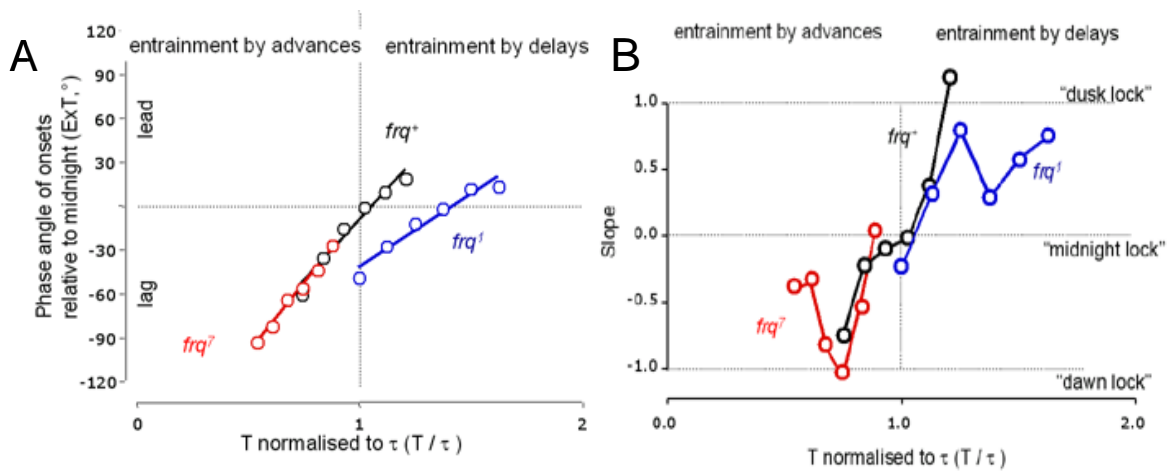


Figure 4.7: Graphical representation of the phase angle of conidiation in long (A) and short (B) photoperiods. **(A)** In long photoperiods, with *N.c.* being entrained to midnight, the phase angle delays more the longer the T-cycle is. On the x-axis the cycle length is related to the FRP of the respective strain, on the y-axis lags and leads are related to midnight. **(B)** In short photoperiods, the coupling of *N.c.* changes with the length of the cycle. X-axis as in (A), the y-axis gives the slope of a line fitted to the onsets of conidiation (with dusk and dawn having a slope of 1 and -1 , respectively). (Graphs by Prof. Roenneberg, personal communication)

Summing up the physiological characteristics of entrainment in *Neurospora crassa*, it is evident that *Neurospora* does entrain to light cycles. It does so in a highly systematic fashion, and even in skeleton photoperiods. Furthermore, the coupling to dusk, dawn and midnight is a behavior so far only shown in higher organisms. Therefore, the results are comparable to entrainment in other organisms, underlining the importance of *Neurospora crassa* as a model organism in circadian research.

Also, this study is the first to describe the phenotype of entrainment comprehensively over so many conditions. Only in model organisms that offer the experimental possibilities of *Neurospora*, is the compiling of so many conditions possible. That allowed establishing rules of entrainment, which in turn allowed choosing the best cycles for molecular experiments to investigate coupling to midnight, dawn and dusk. The results from this thesis can now be used to test the rules of entrainment - that were established for *Neurospora* - in other organisms with fewer experiments. The rules of entrainment do not have to be investigated as extensively as in this study but rather can the rules be tested in other organisms by choosing cycles according to the relationship of the FRP and the cycle length. Furthermore, designing molecular experiments will be more focused, when considering the consequences of a cycle length longer, equal or shorter than the endogenous cycle length of an organism.

4.2. Entrainment on the molecular level

Neurospora entrains to light cycles and a set of simple and highly systematic rules can be deducted. Taking those rules, this thesis then investigated the molecular mechanisms of entrainment. In distinguishing drivenness from entrainment, the kinetics of protein and RNA and their relationship is especially important: In drivenness, uniform responses, irrespective of cycle length and zeitgeber strength, is expected. In entrainment, a systematic change, indicating an active process of synchronization is expected.

In addressing molecular responses to light in *Neurospora*, Crosthwaite and colleagues (1995) have shown, that *frq* RNA is up-regulated within 5 minutes after light reaches dark-grown *Neurospora*. In the concomitant physiological experiments, they showed distinct phase advances in the banding pattern. The conclusion was that the reset by the light stimulus is the molecular correlate of entrainment (Crosthwaite, Loros et al. 1995; Crosthwaite, Dunlap et al. 1997). Our group has shown previously, though, that the kinetics of RNA and protein dissociate in various entrainment protocols and that the peak and trough of RNA levels do not correlate with the changes in the entrained phase angle (Tan, Dragovic et al. 2004). That enhances the notion that a one-time reaction of *Neurospora* as in Crosthwaite's study does not necessarily reflect the complex process of entrainment.

In this study, the sharp up-regulation of mRNA was replicated, not only for *frq*-RNA but also for *vvd*-RNA. What was also replicated from our group's previous

work (Tan, Dragovic et al. 2004) was the dissociation of *frq*-RNA and FRQ-protein kinetics. That, again, was enhanced by the findings for the VVD-protein in this thesis, where a similar dissociation of RNA and protein could be shown.

Furthermore, degradation kinetics seem to play an important role for entrainment. Up-regulation of FRQ is similar in all of the cycles, but the down-regulation is markedly different, with a prolonged elevated level in longer cycles. This is an important aspect for future research, because so far degradation has been addressed in circadian research and it has been shown to be a crucial element in the negative feedback loop (Ashmore and Sehgal 2003; He and Liu 2005), but it has so far not been related to entrainment.

As a conclusion from this study of entrainment in *Neurospora*, protein kinetics seem to be the key component in the mechanism, with the peak of protein levels and the different degradation kinetics accounting for the differences in entrained phase angles.

For future molecular research in general, the physiological experiments should be chosen carefully to allow the studied organisms to fully entrain to zeitgeber cycles. Also experimental conditions need to be chosen carefully to account for the possibility of masking of results (Roenneberg, Dragovic et al. 2005), and to be able to choose the correct cycles for molecular research. Lastly, when analyzing molecular data, all aspects of molecular changes need to be addressed: up-regulation as well as down-regulation.

4.3. Does *Neurospora crassa* have an M&E oscillator?

As shown in this thesis, *Neurospora* is very well suited as a model organism in circadian research. As described above (see section 1.2), the circadian oscillator is the centerpiece of the circadian clock: in terms of mathematical description a sine-oscillator, in terms of molecules a translational-transcriptional feedback loop (or several of them).

This observation is important when evaluating whether *Neurospora* is entrained (a systematic synchronization) instead of being driven (a fixed stimulus-response pattern; Roenneberg, Dragovic et al. 2005). This study showed that *Neurospora crassa* entrains to light cycles in a highly systematic fashion. The data clearly show for the first time in *Neurospora crassa* that entrainment is not uniform in respect to the light-dark transitions, but it rather changes the relationship, i.e. the coupling, to the light-dark cycle, by being coupled to dawn, dusk or midnight. A theory to explain morningness (M) and eveningness (E), i.e. the coupling of the phase angle to dawn or dusk, is the M&E oscillator theory. It proposes the existence of two distinct, non-redundant oscillators with a decisive difference in the way light signals are computed (Pittendrigh and Daan 1976). The dawn (morningness) oscillator is advanced by light and delayed by darkness, the dusk (eveningness) oscillator has reciprocal properties (Daan, Albrecht et al. 2001).

Next to the coupling of the phase angle to dawn and dusk, *Neurospora crassa* fulfills other properties that the M&E model predicts. It changes the length of the activity period α with a changing photo- and scotoperiod.

Two distinct oscillators can explain these different properties of the system. When considering the M&E oscillators in a mammalian circadian system, one question is left open, though: At what level of organization of the mammalian circadian clock is the distinction between the M and the E component made? Is it at the molecular level, with the *per1*, *cry1* and the *per2*, *cry2* complexes forming the two parts (Daan, Albrecht et al. 2001)? Is it at the neuronal level, with different groups of neurons generating multiple unit activities (MUA) at different times (Jagota, Iglesia et al. 2000)? Or even at the anatomical level, with the distinction between different layers or even the two suprachiasmatic nuclei (Jagota, Iglesia et al. 2000)?

The advantage of *Neurospora crassa* in investigating this question is its organization as single cells, a syncytial organism at most. Anatomical distinctions are obviously not possible. But even in the single cell, there are several possibilities for the organization of an M and an E component.

The clear entrainment to dawn, dusk and to midnight could be the physiological behaviour that is founded on M&E oscillators, which could be 2 distinct transcriptional-translational feedback loops (TTL). So far only one loop, the *frq-wc* feedback-loop, is well described in *Neurospora's* clock. A FRQ-less oscillator is proposed, but its components remain elusive (Morrow and Roenneberg 2001). One recent attempt to define a second TTL (Francois 2005), reports the less characterized

enhancement of *white-collar 1* (WC-1) protein synthesis by FRQ as the positive second feedback loop.

The distinction of M&E could also be found in different light receptors, gating light differently at different times of day (Dragovic, Tan et al. 2002), for example the differential gating of light by WC-1 as well as by the VVD protein (Heintzen, Loros et al. 2001). Furthermore, the VVD-protein showed similar kinetics in this study as the FRQ-protein did in previous work (Tan, Dragovic et al. 2004). For both proteins, degradation seems to be an important regulator for entrainment, with protein levels remaining elevated for a longer time, the longer the cycle is chosen.

The M&E response could also be based on entirely different principles, for example two distinct oscillations of redox-changes (Morrow and Roenneberg 2001).

The results from this study can be explained by an M&E oscillator, they fit its criteria, but the generation of these two distinct oscillations remains only partly understood, and opens many possibilities for future research.

A future goal of circadian research will be to assemble one complete model of the molecular mechanisms of a circadian clock from input over central oscillations to output. *Neurospora* could well be used to describe that first complete clock, because despite its cellular-syncitial organization, this thesis shows for the first time a circadian behavior as complex as in higher organisms with the extraordinary benefit of an easily accessible research organism.

5. Summary

Circadian rhythms influence almost every process in almost every organism. Understanding circadian rhythmicity is a crucial tool to understand many other biological processes. In this study *Neurospora crassa*, a filamentous fungus, was used to investigate the synchronization of internal time and external light-dark cycles (light entrainment).

For physiology experiments a circadian surface was done, taking light-dark cycles of different lengths and varying the ratio of light to dark within each cycle. A highly systematic response could be seen: In cycles shorter than the free running period (FRP), conidiation in *N. crassa* entrains to dawn, in cycles with a length around the FRP conidiation entrains to midnight, and in cycles longer than the FRP conidiation entrains to dusk. This shows that *N.c.* entrains to light-dark cycles rather than to be driven by them. Additionally, *N.c.* entrains even to skeleton photoperiods with characteristics similar to other, higher, organisms. The results allowed to deduct a set of simple and highly systematic rules for entrainment to light, which can now be tested in higher organisms with less experimental effort.

After entrainment on the physiology level was shown, the next step in this thesis was to investigate the mechanisms on the molecular level. Here a replication and enhancement of previous results was shown: The quick up-regulation of RNA after lights-on was repeated. Further repeating previous results, protein kinetics were shown to not be uniformly coupled to RNA-kinetics. Enhancing previous

results, protein degradation seems to play an important role in entrainment, changing systematically with the varying entrainment protocols.

Circadian research has been focused on the free-running period. In the future, entrainment - as an expression of the active process of zeitgeber computation by the circadian clock - will be studied more closely to understand the clock wheels of the circadian system. With this thesis it was shown that even a simple organism like *Neurospora crassa* entrains to light cycles rather than to be merely driven, and it entrains with characteristics that are comparable to higher organisms. This underlines the usefulness of *Neurospora crassa* as a model organism in circadian research, and lays the ground for entrainment research in higher organisms.

6. Zusammenfassung

Circadiane Rhythmen beeinflussen fast jeden biologischen Prozess in fast jedem Organismus. Das Verständnis von circadianen Rhythmen ist entscheidend um viele andere biologische Prozesse zu verstehen. In dieser Doktorarbeit wurde der Sprosspilz *Neurospora crassa* benutzt um die Synchronisation von innerer Uhr mit Hell-Dunkel Zyklen zu untersuchen (Licht-„Entrainment“).

Durch physiologische Experimente wurde eine circadiane Oberfläche erstellt, indem die Sporulation von *Neurospora crassa* in Licht-Dunkel-Zyklen verschiedener Länge mit unterschiedlichen Licht-Dunkel-Verhältnissen innerhalb der einzelnen Zyklen analysiert wurde. Das Verhalten von *Neurospora* war sehr systematisch: In Lichtzyklen, die kürzer als der innere Tag waren, synchronisierte sich die Sporulation bei *N. crassa* relativ zur Morgendämmerung (Licht an), in Zyklen die in etwa der inneren Uhrlänge entsprachen synchronisierte sie sich zu Mitternacht, und in Zyklen die länger waren zur Abenddämmerung (Licht aus). Dies zeigte, dass sich *N.c.* aktiv mit Licht-Dunkel-Zyklen synchronisiert anstatt nur auf sie zu reagieren. Zusätzlich konnte gezeigt werden, dass *N.c.* sich sogar mit skelettierten Licht-Dunkel-Zyklen (Die Licht-an und die Licht-aus-Grenze wurden durch 2-stündige Lichtpulse simuliert) aktiv synchronisiert, und zwar mit einer Systematik die in höheren Organismen schon beschrieben wurde. Mit diesen Ergebnissen konnten einfache aber sehr systematische Regeln für circadiane Lichtsynchronisation erstellt werden. Diese könne nun wiederum benutzt werden, um Lichtsynchronisation in

höheren Organismen zu untersuchen, bei denen die aufwendigen Experimente dieser Doktorarbeit logistisch nicht möglich sind.

Nachdem die aktive Synchronisation von innerer Uhr und äußeren Zeitgebern gezeigt wurde, wurden in dieser Doktorarbeit die molekularen Mechanismen der Synchronisation von innerer und äußerer Zeit untersucht. Es konnten vorherige Ergebnisse repliziert und erweitert werden: Die schnelle Hoch-Regulierung von RNA durch das Lichtsignal wurde bestätigt, ebenso wie die vorherigen Ergebnisse unserer Gruppe, dass RNA-Kinetik und Proteinkinetik nicht linear verbunden sind. Die bekannten Mechanismen wurden erweitert, indem gezeigt wurde, dass Proteinabbau eine wichtige Rolle in der aktiven Synchronisation von innerer und äußerer Zeit spielt, da sie sich systematisch veränderte als die Lichtzyklen systematisch verändert wurden.

Die circadiane Forschung hatte ihren Schwerpunkt bisher auf Versuchen in konstanten Bedingungen. In der Zukunft wird „Entrainment“ (der aktive Synchronisationsprozess von äußerer Zeitinformationen und Zustand der inneren Uhr) in den Mittelpunkt der Forschung treten, um die Arbeit der Zahnräder der inneren Uhr besser zu verstehen. Mit dieser Doktorarbeit konnte gezeigt werden, dass ein einfacher Organismus wie *Neurospora crassa* sich aktiv mit Lichtzyklen synchronisiert anstatt nur auf sie zu reagieren, und das mit Charakteristika, die dem Verhalten von höheren Organismen entsprechen. Das zeigt den Nutzen von *Neurospora crassa* als Modellorganismus in der circadianen Forschung und ermöglicht systematischere „Entrainment“-Forschung in höheren Organismen.

7. References

1. Allada, R. (2003). "Circadian clocks: a tale of two feedback loops." Cell **112**(3):329-41
2. Aronson, B. D., K. A. Johnson, et al. (1994). "The circadian clock locus *frequency*: a single ORF defines period length and temperature compensation." Proc Natl Acad Sci USA **91**: 7683-7687.
3. Aschoff, J. (1965). "Circadian rhythms in man." Science **148**: 1427-1432.
4. Aschoff, J. (1985). "On the perception of time during prolonged isolation." Human Neurobiol **4**(time perception): 41-52.
5. Ashmore, L. and A. Sehgal (2003). "A fly's eye view of circadian entrainment." J Biol Rhythms **18**(3): 206-16.
6. Beck, S. D. (1962). "Photoperiodic induction of diapause in an insect." Biological Bulletin **122**(1): 1-12.
7. Berson, D. M., F. A. Dunn, et al. (2002). "Phototransduction by retinal ganglion cells that set the circadian clock." Science **295**(5557): 1070-3.
8. Bieszke, J., E. Spudich, et al. (1999). "A eukaryotic protein, NOP-1, binds retinal to form an archaeal rhodopsin-like photochemically reactive pigment." Biochemistry **38**(43): 14138-45.
9. Bognar, L. K., A. H. Adam, et al. (1999). "The circadian clock controls the expression pattern of the circadian input photoreceptor, *phytochrome B*." Proc Natl Acad Sci USA **96**: 14652-14657.
10. Bruce, V. (1960). "Environmental Entrainment of Circadian Rhythms." Cold Spring Harbor Symp Quant Biol **25**: 29-47.
11. Covic, A. and D. Goldsmith (1999). "Ambulatory blood pressure monitoring in nephrology: focus on BP variability." J Nephrol **12**(4): 220-9.
12. Crosthwaite, S. K., J. C. Dunlap, et al. (1997). "*Neurospora wc-1* and *wc-2*: Transcription, photoresponses, and the origin of circadian rhythmicity." Science **276**: 763-769.
13. Crosthwaite, S. K., J. J. Loros, et al. (1995). "Light-induced resetting of a circadian clock is mediated by a rapid increase in *frequency* transcript." Cell **81**: 1003-1012.
14. Daan, S., U. Albrecht, et al. (2001). "Assembling a clock for all seasons: are M and E oscillators in the genes?" J Biol Rhythms **16**(2): 105-116.
15. Daan, S., M. Merrow, et al. (2002). "External time - internal time." J Biol Rhythms **17**(2): 107-109.
16. Darwin, C. (1880). On the power of movement in plants. London, John Murray.
17. DeCoursey, P., J. Walker, et al. (2000). "A circadian pacemaker in free-living chipmunks: essential for survival?" J Comp Physiol **186**(2): 169-80.
18. Denault, D. L., J. J. Loros, et al. (2001). "WC-2 mediated WC-1-FRQ interaction within the PAS protein-linked circadian feedback loop of *Neurospora*." EMBO J **20**: 109-117.

19. Diernfellner, A., T. Schafmeier, et al. (2005). "Molecular mechanism of temperature sensing by the circadian clock of *Neurospora crassa*." Genes Dev **19**(17): 1968-73.
20. Dragovic, Z., Y. Tan, et al. (2002). "Light reception and circadian behavior in 'blind' and 'clock-less' mutants of *Neurospora crassa*." EMBO J **21**: 3643-3651.
21. Eastman, C., M. Young, et al. (1998). "Bright light treatment of winter depression: a placebo-controlled trial." Arch Gen Psychiatry **55**(10): 883-9.
22. Ebisawa, T., M. Uchiyama, et al. (2001). "Association of structural polymorphisms in the human period3 gene with delayed sleep phase syndrome." EMBO Rep **2**(4): 342-6.
23. Feldman, J. F. and M. N. Hoyle (1973). "Isolation of circadian clock mutants of *Neurospora crassa*." Genetics **75**: 605-613.
24. Francois, P. (2005). "A model for the *Neurospora* circadian clock." Biophys J **88**(4): 2369-83.
25. Freedman, M. S., R. J. Lucas, et al. (1999). "Non-rod, non-cone ocular photoreceptors regulate the mammalian circadian behaviour." Science **284**(5413): 502-504.
26. Froehlich, A. C., Y. Liu, et al. (2002). "White Collar-1, a circadian blue light photoreceptor, binding to the *frequency* promoter." Science **297**: 815-819.
27. Galagan, J., S. Calvo, et al. (2003). "The genome sequence of the filamentous fungus *Neurospora crassa*." Nature **422**(6934): 821-2.
28. Goldman, B. (1999). "The Siberian hamster as a model for study of the mammalian photoperiodic mechanism." Adv Exp Med Biol **460**: 155-64.
29. Goldman, B. (2001). "Mammalian photoperiodic system: formal properties and neuroendocrine mechanisms of photoperiodic time measurement." J Biol Rhythms **16**(4): 283-301.
30. Gwinner, E. (1986). Circannual rhythms. Berlin, Springer Verlag.
31. Hankins, M. W. and R. J. Lucas (2002). "A novel photopigment in the human retina regulates the activity of primary visual pathways according to long-term light exposure." Curr Biol **12**(3): 191-198.
32. Hattar, S., H. W. Liao, et al. (2002). "Melanopsin-containing retinal ganglion cells: architecture, projections, and intrinsic photosensitivity." Science **295**: 1065-1070.
33. He, Q. and Y. Liu (2005). "Degradation of the *Neurospora* circadian clock protein FREQUENCY through the ubiquitin-proteasome pathway." Biochem Soc Trans **33**: 953-6.
34. Heintzen, C., J. J. Loros, et al. (2001). "The PAS Protein VIVID Defines a Clock-Associated Feedback Loop that Represses Light Input, Modulates Gating, and Regulates Clock Resetting." Cell **104**: 453-464.
35. Hurst, W., J. Mitchell, et al. (2002). "Synchronization and phase-resetting by glutamate of an immortalized SCN cell line." Biochem Biophys Res Commun **298**(1): 133-43.
36. Jagota, A., H. d. I. Iglesia, et al. (2000). "Morning and evening circadian oscillations in the suprachiasmatic nucleus in vitro." Nat Neurosci **3**(4): 372-6.

37. Johnson, C. and S. Golden (1999). "Circadian programs in cyanobacteria: adaptiveness and mechanism." Annu Rev Microbiol **53**: 389-409.
38. Kawachi, I., G. A. Colditz, et al. (1995). "Prospective study of shift work and risk of coronary heart disease in women." Circulation **92**: 3178-3182.
39. Lee, K., J. C. Dunlap, et al. (2003). "Roles for WHITE COLLAR-1 in circadian and general photoreception in *Neurospora crassa*." Genetics **168**: 103-114.
40. Lee, K., J. J. Loros, et al. (2000). "Interconnected feedback loops in the *Neurospora* circadian system." Science **289**: 107-110.
41. Liu, Y. (2003). "Molecular mechanisms of entrainment in the *Neurospora* circadian clock." J Biol Rhythms **18**(3): 195-205.
42. Liu, Y., N. Garceau, et al. (1997). "Thermally regulated translational control of FRQ mediates aspects of temperature responses in the *neurospora* circadian clock." Cell **89**(3): 477-86.
43. Loros, J. and J. Feldman (1986). "Loss of temperature compensation of circadian period length in the *frq-9* mutant of *Neurospora crassa*." J Biol Rhythms **1**(3): 187-98.
44. Loros, J. J. and J. C. Dunlap (2001). "Genetic and molecular analysis of circadian rhythms in *Neurospora*." Annu Rev Physiol **63**: 757-794.
45. Loros, J. J. and J. F. Feldman (1986). "Loss of temperature compensation of circadian period length in the *frq-9* mutant of *Neurospora crassa*." J Biol Rhythms **1**: 187-198.
46. Loudon, A. S., N. Ihara, et al. (1998). "Effects of a circadian mutation on seasonality in Syrian hamsters (*Mesocricetus auratus*)." Proc R Soc Lond B Biol Sci **265**(1395): 517-521.
47. Lüttge, U. (2000). "The tonoplast functioning as the master switch for circadian regulation of crassulacean acid metabolism." Planta **211**: 761-769.
48. Menaker, M. (2003). "Circadian rhythms. Circadian photoreception." Science **299**(5604): 213-4.
49. Mellow, M., M. Brunner, et al. (1999). "Assignment of circadian function for the *Neurospora* clock gene *frequency*." Nature **399**: 584-586.
50. Mellow, M., L. Franchi, et al. (2001). "Circadian regulation of the light input pathway in *Neurospora crassa*." EMBO J **20**(3): 307-315.
51. Mellow, M. and T. Roenneberg (2001). "Circadian clocks: running on redox." Cell **106**: 141-143.
52. Mellow, M. and T. Roenneberg (2001). "The circadian cycle: is the whole greater than the sum of its parts?" TIGS **17**: 4-7.
53. Mellow, M. W. and J. C. Dunlap (1994). "Intergeneric complementation of a circadian rhythmicity defect: phylogenetic conservation of structure and function of the clock gene *frequency*." EMBO J **13**: 2257-2266.
54. Moore-Ede, MC (1986) "Jet lag, shift work, and maladaptation." NIPS **1**:156-160.
55. Mormont, M. and F. Levi (2003). "Cancer chronotherapy: principles, applications, and perspectives." Cancer **98**(4): 881-2.

56. Oishi, K., K. Miyazaki, et al. (2003). "Genome-wide expression analysis of mouse liver reveals CLOCK-regulated circadian output genes." J Biol Chem **278**(42): 41519-27.
57. Oren, D., K. Wisner, et al. (2002). "An open trial of morning light therapy for treatment of antepartum depression." Am J Psychiatry **159**(4): 666-9.
58. Pittendrigh, C. S. (1954). "On temperature independence in the clock controlling emergence time in *Drosophila*." Proc Natl Acad Sci USA **40**: 1018-1029.
59. Pittendrigh, C. S. (1960). "Circadian rhythms and the circadian organization of living systems." Cold Spring Harbor Symp Quant Biol **25**: 159-184.
60. Pittendrigh, C. S. and S. Daan (1976). "A functional analysis of circadian pacemakers in nocturnal rodents: V. Pacemaker structure: a clock for all seasons." J Comp Physiol A **106**: 333-355.
61. Pittendrigh, C. S. and S. Daan (1976a). "A functional analysis of circadian pacemakers in nocturnal rodents: I. The stability and lability of circadian frequency." J Comp Physiol A **106**: 223-252.
62. Reinberg, A., P. Andlauer, et al. (1984). "Desynchronization of the oral temperature circadian rhythm and intolerance to shift work." Nature **308**: 272-274.
63. Reppert, S. M. and D. R. Weaver (2002). "Coordination of circadian timing in mammals." Nature **418**: 935-941.
64. Richter, C. (1978). "Evidence for existence of a yearly clock in surgically and self-blinded chipmunks." Proc Natl Acad Sci USA **75**(7): 3517-3521.
65. Roden, M., M. Koller, et al. (1993). "The circadian melatonin and cortisol secretion pattern in permanent shift workers." Am J Physiol **265**: R261-R267.
66. Roenneberg, T., S. Daan, et al. (2003). "The art of entrainment." J Biol Rhythms **18**(3): 183-194.
67. Roenneberg, T., Z. Dragovic, et al. (2005). "Demasking biological oscillators: Properties and principles of circadian entrainment exemplified by the *Neurospora* circadian clock." Proc Natl Acad Sci USA **102**(21): 7742-7747.
68. Roenneberg, T. and R. Foster (1997). "Twilight times: light and the circadian system." Photochem Photobiol **66**(5): 549-61.
69. Roenneberg, T. and M. Meroow (1998). "Molecular circadian oscillators - an alternative hypothesis." J Biol Rhythms **13**: 167-179.
70. Roenneberg, T. and M. Meroow (2000). "Circadian light input: omnes viae Romam ducunt." Curr Biol **10**: R742-R745.
71. Roenneberg, T. and M. Meroow (2001). "Seasonality and photoperiodism in fungi." J Biol Rhythms **16**: 403-414.
72. Roenneberg, T. and M. Meroow (2002). "Life before the clock - modeling circadian evolution." J Biol Rhythms **17**(6): 495-505.
73. Roenneberg, T. and D. Morse (1993). "Two circadian oscillators in one cell." Nature **362**: 362-364.
74. Roenneberg, T., A. Wirz-Justice, et al. (2003). "Life between clocks - daily temporal patterns of human chronotypes." J Biol Rhythms **18**(1): 80-90.

75. Sack, R. L., A. J. Lewy, et al. (1991). "Melatonin administration to blind people: phase advances and entrainment." J Biol Rhythms **6**: 249-262.
76. Sargent, M. L. and S. H. Kaltenborn (1972). "Effects of medium composition and carbon dioxide on circadian conidiation in *Neurospora*." Plant Physiol **50**: 171-175.
77. Schafmeier, T., A. Haase, et al. (2005). "Transcriptional feedback of *Neurospora* circadian clock gene by phosphorylation-dependent inactivation of its transcription factor." Cell **122**(2): 235-46.
78. Schernhammer, E., F. Laden, et al. (2001). "Rotating night shifts and risk of breast cancer in women participating in the nurses' health study." J Natl Cancer Inst **93**(20): 1563-8.
79. Schernhammer, E., F. Laden, et al. (2003). "Night-shift work and risk of colorectal cancer in the nurses' health study." J Natl Cancer Inst **95**:825-8.
80. Schwartz, W., H. d. l. Iglesia, et al. (2001). "Encoding le quattro stagioni within the mammalian brain: photoperiodic orchestration through the suprachiasmatic nucleus." J Biol Rhythms **16**(4): 302-11.
81. Schwartz, W. J. and H. Gainer (1977). "Suprachiasmatic nucleus: use of C- labeled deoxyglucose uptake as a functional marker." **97**: 89-109.
82. Schwerdtfeger, C. and H. Linden (2003). "VIVID is a flavoprotein and serves as a fungal blue light photoreceptor for photoadaptation." EMBO J **22**(18): 4846-55.
83. Silver, R., A. Sookhoo, et al. (1999). "Multiple regulatory elements result in regional specificity in circadian rhythms of neuropeptide expression in mouse SCN." Neuroreport **10**(15): 3165-74.
84. Somers, D. E., P. F. Devlin, et al. (1998). "Phytochromes and cryptochromes in the entrainment of the *Arabidopsis* circadian clock." Science **282**: 1488-1490.
85. Tan, Y., Z. Dragovic, et al. (2004). "Entrainment dissociates transcription and translation of a circadian clock gene in *Neurospora*." Curr Biol **14**(5): 433-8.
86. Tan, Y., M. Meroz, et al. (2004). "Photoperiodism in *Neurospora crassa*." J Biol Rhythms **19**(2): 135-143.
87. Terman, M., A. Lewy, et al. (1995). "Light treatment for sleep disorders: consensus report. IV. Sleep phase and duration disturbances." J Biol Rhythms **10**(2): 135-47.
88. Towbin, H., T. Staehelin, et al. (1979). "Electrophoretic transfer of protein from polyacrylamid gels to nitrocellulose sheets: procedure and some applications." Proc Natl Acad Sci USA **79**: 267-271.
89. Welsh, D. K., D. E. Logothetis, et al. (1995). "Individual neurons dissociated from rat suprachiasmatic nucleus express independently phased circadian firing rhythms." Neuron **14**: 697-706.

8. Appendix:

8.1. Abbreviations

μ	Micro (10^{-6})
A	Ampere
aa	amino-acid
bp	base pairs
cDNA	Complementary DNA
DD	Constant darkness
DNA	Deoxyribonucleic acid
dNTP	Deoxynucleoside triphosphate
E (/sec/m ²)	Einstein, 1 mol photons (per second and m ²)
FGSC	also "fgsc", Fungal Genetic Stock Centre
FRP	Free running period = τ
<i>frq</i>	<i>frequency</i> gene
FRQ	<i>frequency</i> gene product (FRQ protein)
g	Gram
h	Hour
HEPES	4-(2-hydroxyethyl)-1-piperazineethanesulfonic acid buffer
IgG	Immunoglobulin G
k	kilo (10^3)
LD	Light-Dark
LL	Constant light
M	Molar
m	milli (10^{-3})
min	Minute
mRNA	messenger ribonucleic acid
n	nano (10^{-9})

NTP	Nucleoside triphosphate
OD	optical density
PAGE	Polyacrilamide gel electrophoresis
PCR	Polymerase Chain Reaction
PMSF	Phenyl-methyl-sulfonyl-fluoride
RNA	Ribonucleic acid
RT-PCR	Real Time Polymerase Chain Reaction
SCN	supra chiasmatic nucleus
τ	free running period, FRP
Taq	<i>Thermophilus aquaticus</i> DNA polymerase
UTP	Uridine-triphosphate
V	Volt
<i>vvd</i>	<i>vivid</i> gene
VVD	<i>vivid</i> gene product (VVD protein)
V/V	Volume per volume
w/V	Weight per volume
<i>wc-1</i>	<i>white collar-1</i> gene
WC-1	<i>white collar-1</i> gene product (WC-1 protein)
<i>wc-2</i>	<i>white collar-2</i> gene
WC-2	<i>white collar-2</i> gene product (WC-2 protein)
wl	wavelength
<i>wt</i>	wild type

8.2. Recipes

- Acrylamide solution

Acrylamide	29.2 g
N, N'-Methylene-bis-acrylamide	0.8 g
ddH ₂ O	Up to 100 ml

- Blotting buffer

TRIS	50mM
Glycin	384mM
Methanol	20% (V/V)

- Buffer for semi-dry blot

Glycin	14.4 g
Tris	3 g
Methanol	200 ml
ddH ₂ O	up to 1000ml

- Electrophoresis buffer (SDS Page) 10X

Glycin	144.13 g
TRIS	30.28 g
SDS	10 g
ddH ₂ O	up to 1000ml

- PBS 10X

NaCl	80 g
KCl	2 g
Na ₂ HPO ₄ x 7H ₂ O	11.5 g
K ₂ HPO ₄	2 g
ddH ₂ O	up to 1000ml

- Laemmle Buffer

TRIS/HCl pH6.8	60mM
SDS	2% (w/V)
b-Mercaptoethanol	5% (w/V)
Glycerol	10% (w/V)
Bromophenol Blue	0.2% (w/V)

- Ponceau solution

Ponceau	0.2% (w/V)
Trichloroacetic acid	3% (w/V)

- Protein dephosphorylation buffer 1X

HEPES/KOH pH 7.4	50 mM
NaCl	137 mM
Glycerin	10% (v/v)
EDTA	5 mM
PMSF	1 mM l
Leupeptin	1 µg/ml
Pepstatin A	1 µg/ml

- Protein extraction buffer (PEB)

Hepes	1.2g
Glycerol	10ml
NaCl (5M)	2.7ml
EDTA (0.5M, pH 8.0)	1ml
H ₂ O	90ml

- Race tube media

Bacto-Agar	2% (w/V)
Arginine	0.5% (w/V)
Glucose	0.3% (w/V)
Vogel's salts	1X
Biotin	1ng/ml

- RNA extraction buffer

EDTA (0.5M, pH 8.0)	2ml
TRIS (1M, pH 8.0)	10ml
SDS (10%)	40ml
NaCl (5M)	12ml
H ₂ O	36ml

- Standard trace element solution

H ₃ BO ₃ (anhydrous)	0.05g/l
CuSO ₄ . 5H ₂ O	0.25g/l
Fe(NH ₄) ₂ (SO ₄) . 6H ₂ O	1.0g/l
MnSO ₄ . 5H ₂ O	0.05g/l
ZnSO ₄ . 7H ₂ O	5.0g/l
Na ₂ MoO ₄ . 2H ₂ O	0.05g/l
Citric Acid . H ₂ O	5.0g/l

- TBS 10X

NaCl	90g
TRIS 1M, pH 7.4	200ml
Tween 20 (20%)	2.5ml
H ₂ O	fill up to 1000ml

- Vogel's liquid medium (for mycelial mats)

Glucose	2.0% (w/V)
Arginine	0.5% (w/V)
Vogel's salts	1X
Biotin	1ng/ml

- Vogel's minimal agar medium (for slants)

Glucose	2%
Bacto-Agar	2%
Vogel's salts	1X

- 50X Vogel's salts

H ₂ O	750ml
Na ₃ Citrate . 5.5 H ₂ O (2 H ₂ O)	150g (125g in 775ml ddH ₂ O)
KH ₂ PO ₄ (anhydrous)	250g
NH ₄ NO ₃ (anhydrous)	100g
MgSO ₄ . 7 H ₂ O	10g (4.88g MgSO ₄)
CaCl ₂ . 2 H ₂ O (0 H ₂ O)	5g (3.8g)
Trace elements solution	5.0 ml
Biotin (0,1mg/ml)	2.5ml
H ₂ O	750ml

pH is adjusted to 5.8 with HCl and NaOH

Chloroform (2ml) is added for preservation

8.3. List of Instruments

Autoclave, type 300, Varioklav

Blotting apparatus, Trans-Blot cell (with plate electrodes), BioRad

Blotting apparatus, custom made; Specification: Helmut Klausner, workshop of IMP, Goethestr.
31/U1, 80336 Munich, Germany

Centrifuge, 5415C, Eppendorf

Centrifuge, 5417R, Eppendorf

Centrifuge, Biofuge Primo-R, Heraeus

Electrophoresis apparatus, vertical (gel size 120x140x0.75, 1.00 or 1.50mm) and horizontal (for
DNA and RNA, gel size 5x7.5, 9x7.5, 11x14 and 14x23 cm) all custom made; Specification:

Helmut Klausner, workshop of Inst. f. Med. Psych. Goethestr. 31/U1, 80336 Munich, Germany

Electrophoresis apparatus, Mini Protean II cell, BioRad

Electrophoresis apparatus, Protean II xi cell, BioRad

Freezer, -20°C, different models for household

Freezer, -80°C, Heraeus

Magnetic mixer, Ikamag, Junke&Kunkel-Ikawerk

Pipet, with positive displacement, Biomaster, Eppendorf

Pipets, Pipetman (10,20,100,200,1000µl), Gilson

Pipets, Reference (10,20,100,1000,2500µl), Eppendorf

Real Time PCR system, ABI PRISM 7000, Applied Biosystems

Racetubes, Glasbläserei Höhn, München & Glasbl. Schmitz, München

Scale, Handy H 110, Sartorius

Scale, L2200S Sartorius

Scale, Mettler, AE 50, Mettler,

Scintillation counter, LS 1801, Beckman

Shaker, KL2, Bachofer

Shaker, LS10, Gerhard

Spectrophotometer, DU64, Beckman

Spectrophotometer, Ultrospec 3000, Pharmacia

Speed-Vac, Bachofer

Thermal cycler, Primus, MWG Biotech

Thermomixer, 5436, Eppendorf

Thermomixer, comfort, Eppendorf

Timers, WB-388 and TR-118, Oregon Scientific;

Vortex, k-550-GE, Bender&Hobein AG

8.4. List of chemicals

Substance	Company	Order N°.
Acetic Acid	SIGMA	A-6283
Acetone	ALDRICH	17,997-3
Acrylamide	APPLICHEM	A3705,0500
Acrylamide	GERBU	1002
Agarose LOW EEO	APPLICHEM	A2114,0500
Agarose QA TM	Q-BIOGEN	AGR0050
Albumin Bovine	SIGMA	A-3350
Ammonium acetate	SIGMA	A-1542
Ammonium chloride	SIGMA	A-4514
Ammonium nitrate	SIGMA	A-1308
Ammonium peroxodisulfate (APS)	ROTH	9592.3
Ammonium sulfate	ALDRICH	22.125-2
Arginine hydrochlorid (L+)	USB	US 11500
Bacto Agar	DIFCO	214010
Bis acrylamide	SIGMA	M-7279
Boric acid	APPLICHEM	A2940,1000
Boric acid	APPLICHEM	A3581,0500
Calcium chloride x 2H ₂ O	ROTH	5239.1
Chloroform	SIGMA	C-5312
Chloroform:isoamylalcohol	SIGMA	C-0549
Citric acid	ALDRICH	24,062-1
Coomassie brilliant blue	SIGMA	B-0149
Ethanol	ROTH	9065.2
Glucose monohydrate	MERCK	1.04074
Glycerol	APPLICHEM	A2926,1000
Hepes	SIGMA	H-3375
Hexane	ALDRICH	29,325.30

Isoamylalcohol	ROTH	8930.1
Leupeptin	USB	18413
Magnesiumchlorid x 6H ₂ O	MERCK	1.05835.0500
Methanol	ROTH	4627.1
Pepstatin A	USB	US20037
Phenol (DNA/RNA)	ROTH	A.156.1
Phenol (RNA)	ROTH	A.980.1
Phenylmethanesulfonyl fluoride (PMSF)	FLUKA	78830
Polyethyleneglycol PEG 4000	ROTH	156.1
Ponceau S	FLUKA	81460
Potassium chloride	SIGMA	P-3911
Sand	SIGMA	S-9887
SDS / Sodium Dodecyl Sulfate	ROTH	2326.2
Sodium azide	SIGMA	S-2002
Sodium chloride	MERCK	1.06404
Sodium chloride	APPLICHEM	A2942,1000
Sodium citrate	ROTH	3580.1
Sodium dihydrogenphosphate	MERCK	6346
Sodium hydroxid	ROTH	6771.1
Sodium nitrate	FLUKA	71755
Sodium nitrit	ALDRICH	20,783-7
Temed	SIGMA	T-8133
Trichloroacetic acid	SIGMA	T-4885
Tris	APPLICHEM	A1086,100
Tween 20	USB	20605

8.5. List of Biochemicals

Name	Company	Cat No
Alkaline Phosphatase, Calf Intestinal (CIP)	NEBL	M 0290 L
α -Mouse polyvalent immunoglobulins	SIGMA	A-0412
Phosphatase (CIP)	ROCH	776785
dNTPmix	AB	N8080260
PCR system, Exp. Long Template	ROCHE	1-681-842
Protein Assay (Bradford)	BIORAD	500-0006
Protein Assay (gamma glob. standard)	BIORAD	500-005
Protein Markers (pre-stained ladder)	BIORAD	161-0373
Reverse Transcription reagents	AB	N8080234
Reverse Transcriptase	AB	4311235
RNA polymerase	PROMEGA	P2075
RNA Secure	AMBION	7005
RNAguard RNase inhibitor	AMERSHAM	27-0815-01
SYBR Green PCR master mix	AB	4309155
Western Blotting sub. ECL	ROCHE	2015196

9. Acknowledgements – Danksagung

- I am indebted to my doctoral parents: Till Roenneberg and Martha Merrow. I thank you from all of my heart for introducing me to science, for being an inspiration in curiosity without compromises and for allowing a medical student to linger around your habitat for a while. Thank you for your patience and your warm reception. You will always be my standard for true scientists.

- Ich danke Professor Ernst Pöppel für die wissenschaftliche Umgebung, die er in seinem Institut bereitet hat, in der Studenten ihre Forschung gestalten und als Wissenschaftler wachsen können.

- Ich danke den Laborassistentinnen des Roenneberg'schen Labors: Vera Schiewe, Elfie Henoch and Astrid Bauer für die konzentrierte und exakte Arbeit, die die Basis für unsere Erfolge ist.

- Helmut Klausner: Vielen Dank für die exzellente Arbeit beim Bau unserer Forschungsmittel.

- Allen Angestellten am Institut für Medizinische Psychologie: Danke für Eure Freundlichkeit und die schöne Atmosphäre.

- Zdravketina Dragovic: Hvala. I thank you for your introduction to and your teaching of molecular biology. Your exactness in experimental science will be hard to achieve for anyone. Also thank you for teaching me Serbian derogatory language and making bench work very entertaining.

- Kruno Sveric: Ohne Dich wäre ich verhungert und hätte verlernt auch mal wieder an Medizin zu denken.

- Conny Bösl: Never was grinding tissue more fun. Please uphold your spirit. Without you lab life is a lot quieter. I am grateful that I could spend time with you and our little orange friend.

- Ich danke meinen Eltern für ihre Geduld und liebevolle Zuwendung. Ohne sie hätte ich nicht einmal Medizin studiert.

- Ich danke Dir, Constanze, für die Unterstützung und Liebe in allen Lebenslagen und für Deine liebevollen Zurechtweisungen.

10. Lebenslauf – curriculum vitae

Jan Rémi, geborener Ricken am 31.01.1977 in Krefeld

Schulbildung:

1987-97 Gymnasium Weilheim

1994/95 Austauschjahr an der Maroa-Forsyth Highschool in Illinois/USA

Medizinische Ausbildung:

1997/98 Zivildienst (Individuelle Schwerstbehinderten-Betreuung)

1998 - 2005 Studium der Humanmedizin an der LMU München

Praktisches Jahr (April 2004 –März 2005)

1. Tertial: Innere Medizin an der Harvard Medical School
Stipendium der Munich-Harvard Educational Alliance
2. Tertial: Neurologie in der Neurologische Klinik Großhadern
3. Tertial: Chirurgie in der Chirurgische Klinik Innenstadt

Seit Juni 2005: Assistenzarzt in der Neurologischen Klinik und Poliklinik der LMU München

Wissenschaftliche Ausbildung:

- Seit Juni 2000 Mitarbeit als medizinischer Doktorand in der Arbeitsgruppe Prof. Dr. rer.nat. Roenneberg (Chronobiologie), LMU München
- August 2002 – Januar 2003: Aufenthalt bei Volkswagen in Wolfsburg zur Betreuung der Studie: „Einfluss von Licht auf die Innere Uhr von Schichtarbeitern“
- Seit Juni 2005: wissenschaftlicher Assistent an der Neurologischen Klinik und Poliklinik der LMU München (Forschungsgruppe Schlaf und Epilepsie unter Leitung von Prof. Dr. med. S. Noachtar)